Late Cenozoic transpression at the plate boundary: Kinematics of the eastern segment of the Dauki Fault Zone (Bangladesh) and tectonic evolution of the petroliferous NE Bengal Basin

Md. Sakawat Hossain [a], Md. Sharif Hossain Khan [a], Rashed Abdullah [a], Soumyajit Mukherjee [b,*]

[a] Department of Geological Sciences, Jahangirnagar University, Dhaka, 1342, Bangladesh
[b] Department of Earth Sciences, Indian Institute of Technology Bombay, Powai, Mumbai, 400 076, Maharashtra, India

ABSTRACT

The Sylhet Trough in the Bengal Basin (Bangladesh) hosts a number of gas fields. The evolution of the trough is closely associated presumably with the growth and the tectonics of the Dauki Fault Zone (DFZ). Hence understanding the transpression tectonics of the NE Bengal Basin is crucial in petroleum geoscience. The eastern segment of the DFZ in the NE Bengal Basin transpressed dextrally and activated since the latest Miocene up to the earliest Pliocene due to compression along the north, east and southeast. The structural and the tectonic elements of the area are assessed from geomorphic features and deformation structures. Nature of faults and comparison of fault-slip stress field with modern geodetic measurement allow establishing geometric and kinematic relationship between different tectonic elements with the DFZ. Bedding attitude measurements from the study area indicate sub-horizontal east–west-trending antiform fold axis gently plunging towards west confirming the existence of a large-scale monocline. Out of the two interpreted compression directions N–S and E-W, the former explains the orientation of the monocline while the later may cause the dextral transpression in combination with the former compression direction. Fault kinematics and incremental strain axes indicate a bulk north-trending subhorizontal shortening and vertical thickening of the fold and faults approximately perpendicular to the east-west oriented DFZ. The timing of the compressional deformation and fault activation in the study area is inconclusive. Paleostress analyses results match with the present day stress regime and this implies that all the deformations are genetically linked with the DFZ.

1. Introduction

Transpression is a widespread phenomenon in orogenic belts giving rise to complex deformation patterns (e.g., review of Dewey et al., 1998; review of Lin et al., 1999; Pan-African Orogen - Goscombe et al., 2005; Dutta and Mukherjee 2021). It is a kind of strike-slip deformation that deviate from simple shear with shortening oblique to the deformation zone involving a dip-slip component (Lin et al., 1999). This deformation occurs both locally and regionally at plate boundaries and other crustal deformation zones as plates converge obliquely. The resultant deformation structures, e.g., folds, thrusts, positive flower structures, are important in hydrocarbon geosciences (Davison et al., 2015; Nemčok et al., 2016) and seismicity studies (Meghraoui, and Pondrelli, 2012; Benavente et al., 2017).

The Sylhet Trough in the northeastern Bengal Basin (Bangladesh)

occupies a critical geographic position at the junction of three interacting plates-the Indian, the Burmese and the Eurasian plates (e.g., Hiller and Elahi, 1984; Hossain et al., 2014; Hossain et al., 2019). The trough is largely known for being a proven petroleum province (Fig. 1a). The trough formed as the Indian plate rifted and drifted from Antarctica, and was subject to intense sedimentation and deformation in response to the Cenozoic Himalayan orogeny (e.g., Hiller and Elahi, 1984; Hossain et al., 2019).

In the NE Indian Plate, the crustal-scale E-W trending transpressional Dauki Fault Zone (DFZ) (Harris and Beeson, 1993; Hossain et al., 2020a) lies in between two contrasting geologic structures-the uplifting Shillong Plateau to the north and the subsiding Sylhet Trough/Surma basin to the south (Fig. 1). Sylhet Trough is a sub-basin of the central Foredeep part of the Bengal Basin. Genesis of the Sylhet Trough is closely associated with the growth and tectonics of the DFZ and the Shillong Plateau
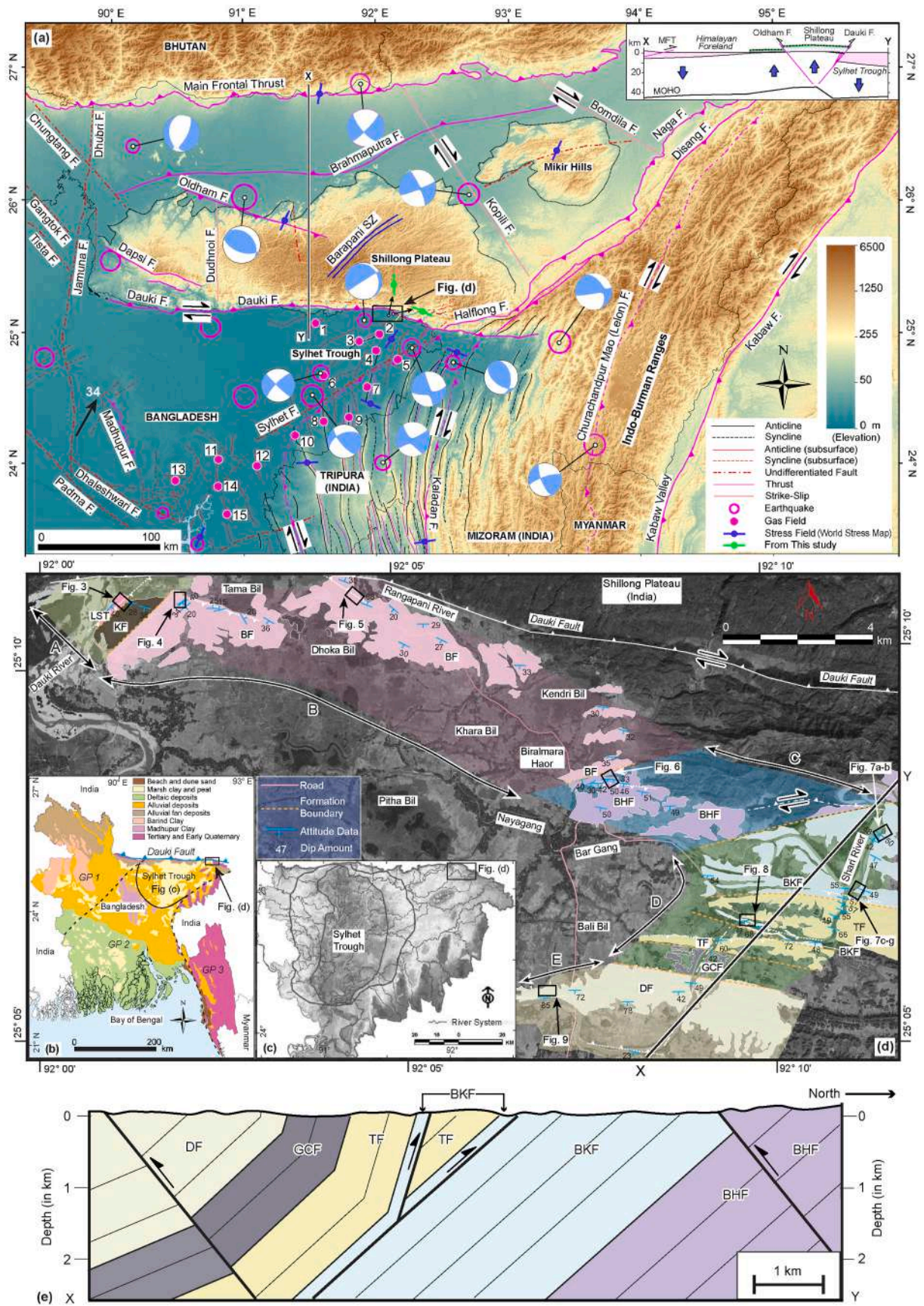
(caption on next page)

Fig. 1. Geologic map of the study area. **(a)** Digital Elevation Model (DEM). Compilations of tectonic features are based on Hossain et al. (2020c). Major earthquakes (Magnitude ≥ 4.5) are marked with hollow pink circles (after Hossain et al., 2019). The radius of the circle represents the earthquake magnitude. Earthquakes focal mechanism are plotted as focal spheres/beach ball diagrams in the NE Himalaya (taken from Bilham and England, 2001; Kumar et al., 2015; Rajendran et al., 2017). Discovered gas fields marked with filled pink circles (after Curiale et al., 2002). Name of the gas fields are marked 1–15 (1 – Chhatak, 2 – Sylhet, 3 – Jalalabad, 4 – Kailas Tila, 5 – Beani Bazar, 6 – Bibiyana, 7 – Fenchuganj, 8 – Rashidpur, 9 – Moulavi Bazar, 10 – Habiganj, 11 – Belabo, 12 – Titas, 13 – Kamta, 14 – Meghna, 15 – Bakhrabad). The gas fields form a ~ NE-oriented zone parallel to the Sylhet Fault. A structural control on hydrocarbon fields (Goffey et al., 2010) looks plausible. Present-day maximum principal stress orientations (σ_1) are taken from the World Stress Map 2016 (Heidbach et al., 2016). Black arrows: GPS-derived direction and magnitude (in mm yr^{-1}) of the present day motion of the India plate with respect to the Shan Block (from Mallick et al., 2019). Simplified N–S (X–Y) cross-section from Biswas et al. (2007). Dark purple arrows represent areas of uplift and subsidence. **(b)** Simplified geological map of Bangladesh. Black dashed lines mark the Geotectonic Province (GP) boundary (modified after Hossain et al., 2020c). **(c)** Drainage map of the Sylhet Trough. Two closed irregular circles at the centre mark the successive deeper portions of the basin (modified after Sarker and Akter, 2011). **(d)** Geo-referenced background panchromatic satellite image taken from the Google Earth Pro. Exposed stratigraphic units, unit boundaries and the major faults marked on the map are picked up by fieldwork during this study. The cross section along the line XY is given in fig. (e). Black rectangle indicates the subsequent figures' locations. Transparent colour shade beneath the exposed formation marked the different studied sections/segments, and labelled A-E (Note: A - Dauki-Mohammadi Segment, B - Tamabil-Naljuri-Sripur Segment, C - Nayagang-Kamalabari Segment, D - Shari River Segment, E – DupiGaon Segment). **(e)** A simplified balanced geologic cross-section along the Shari River section (prepared in this work based on structural constraints of the Shari River section: topography, bedding and fault attitudes, formation boundary, and with the help of Adobe illustrator software). LST – Sylhet Limestone Formation, KF – Kopili Formation, BF – Barail Formation, BHF – Bhuban Formation, BKF – Boka Bil Formation, TF – Tipam Formation, GCF – Girujan Clay Formation, DF – Dupi Tila Formation.

(Biswas and Grasemann, 2005a; Najman et al., 2016). The northern Sylhet Trough (Fig. 1b) falls within a tectonically complex area, involving a N–S shortening (Nielsen et al., 2004; Biswas and Grasemann, 2005b; Steckler et al., 2016) with a component of dextral slip along the E-W-trending DFZ.

The deep-seated DFZ, with a throw >18 km, is traceable in the adjacent country India for ~70 km below sediment cover and has also been identified there as the Garo-Khashi foothill fault system. At least four strands of the DFZ have been identified from the Indian side. Out of these, few are high-angle normal faults, some are high-angle reverse faults, and the rest manifested as monoclines. Locally, the DFZ acted as a tear fault leading to ~300 km translation of the Shillong plateau towards east (review in Nandy, 2001). It might have also acted as a dextral transcurrent fault elsewhere (Sarmah et al., 1992).

The DFZ dips N with a dextral strike-slip component (Johnson and Alam, 1991; Bilham and England, 2001; Biswas and Grasemann, 2005a) and activated since latest Miocene up to the earliest Pliocene (Govin et al., 2018). Others considered the DFZ to be a N-dipping thrust (Dasgupta et al., 2000). The outcrop-level thickness of the DFZ is ~ 5–6 km (Johnson and Alam, 1991). Assuming its dip to be 45° (Bilham and England, 2001; Vernant et al., 2014), the orthogonal thickness of the DFZ would be ~3.89 km. The tectonic development of this crustal-scale fault is directly linked with the N–S shortening as the Indian plate collided against the Eurasian plate. The DFZ is presently more active at the central portion than at its two sides (Biswas and Grasemann, 2005a). Across the DFZ, a significant gradient in gravity anomaly exists (Dasgupta et al., 2000). Also, the fault zone induced mega-scale drag folds towards east, which are located at the south of the DFZ (Fig. 1a). Understanding the kinematics of the DFZ will be crucial since the course of the Brahmaputra River defined by uplift of the Shillong Plateau is controlled by this fault zone. The DFZ also might have resulted in the subsidence of the Sylhet trough, and also be a reason for the 1897 Great Shillong Earthquake (review in Dasgupta et al., 2000).

According to Biswas and Grasemann (2005a), the DFZ is segmented distinctly at its eastern termination. One of these segments of the DFZ continues below the alluvium cover in the northeastern Sylhet Trough, and produces a monocline in the Tertiary sediments (Chowdhury et al., 1996). As the fault is located along the political boundary between Bangladesh and India, its structural synthesis and detailed geophysical survey has remained mostly indeterminate. The impact of Late Cenozoic structural activation(s) along the DFZ on the geometry, kinematics, possible timing of fault activation(s) in the northeastern Sylhet Trough is relatively unknown. Research on these issues can provide a better insight into the tectonic evolution of the trough.

The Sylhet Trough witnessed several major earthquakes in the last few hundred years (Fig. 1a; Bilham, 2004; Hossain et al., 2016, 2019) with epicentres densely located in India (Khattri, 1992; Dasgupta et al.,

2000). Note Nandy (2001) pointed out that instead of DFZ, the Dudhnoi Fault might be a reason of few seismic events. The DFZ has not slipped recently leading to stress build-up. The last rupture of the Dauki Fault occurred in 1897, which produce the Great Indian Earthquake (Oldham, 1899; Yeats et al., 1997). However, if it slips in a single earthquake, it would have catastrophic consequences to the nearby dense population in Bangladesh, Bhutan, India, and Nepal (Hossain et al., 2020b). The 150-km long NE-trending Sylhet Fault (also known as Hail Hakalula Lineament) passes through the SE edge of the Sylhet Trough, is another major fault (Angelier and Baruah, 2009; Hossain et al., 2019). It is probably the southwest extension of the Naga-Disang Thrust, which is offset by the Dauki Fault by its dextral slip component (Ghosh et al., 2015). The November 2017 shallow-focus earthquake (Mw 4.9) in Habiganj, Bangladesh is probably related to the Sylhet Fault.

The Sylhet Trough and its adjacent region hold ~67% of total gas reserves in Bangladesh. Nine out of 20 producing gas fields of Bangladesh are located here (Petrobangla, 2012). Therefore, the interpretation of the fault system and the stress regime are quite important to understand the structure, type, and trend of faults and related fractures. This will significantly impact the location of wells to be drilled, the direction of the well, and the reservoir management to achieve the maximum possible extraction of hydrocarbon.

This article presents a new structural map of the Jaintiapur area in the northeastern Sylhet Trough, almost at the boundary between central and eastern parts of the DFZ. The Jaintiapur and the adjoining areas are bound by the Dauki River at west, the Shari river at east, DFZ at north and in the south by the Shari-Goyain river (Fig. 1d). The study shows evidence for structural deformations and their kinematics in the exposed Cenozoic successions. Structural observations are then constrained by the geomorphic featuresAppendix A related to neotectonics. A NE-SW trending ~10 km long balanced structural cross-section is presented to illustrate the geometry and kinematics of the structures in the subsurface. We also discuss the tectonic evolution of the Sylhet Trough in response to the structural activation(s) along the DFZ. Previous authors based on fieldwork did decipher monoclonal structures from the area. Here we add quantifications, especially in terms of paleostress analyses.

Since fault-plane solutions at the south of the DFZ could not categorically define its kinematics (review: Dasgupta et al., 2000). A field-based investigation of this fault zone would be more conclusive.

2. Geology and stratigraphy

The geologic evolution of the Sylhet Trough is directly related to the collision of the Indian Plate with Eurasian and Burmese plates since Late Eocene that is presently still active (e.g., Hiller and Elahi, 1984; Hossain et al., 2019). Recent GPS-derived geodetic data suggest ~ NNE-directed movement of the NE part of the Indian Plate (central Bengal basin

portion) at 35–40 mm yr^{-1} (Gahalaut et al., 2013; Kreemer et al., 2014; Steckler et al., 2016; Mallick et al., 2019). This modified the sedimentation pattern over the Sylhet Trough (Alam et al., 2003). A rapid influx of clastics from the Himalaya and the Indo-Burman Ranges were deposited during the Miocene. This was followed by a 3-8 times higher than normal rate of subsidence (Johnson and Alam, 1991) of the Sylhet Trough (Alam et al., 2003).

In the northern Sylhet Trough, a major change in sedimentation pattern occurred possibly in the Mid-Pliocene in response to the major thrust-related uplift of the Shillong plateau along the DFZ in the south and Oldham Fault in the north (Johnson and Alam, 1991; Yin et al., 2010; Najman et al., 2016; Govin et al., 2018). These tectonic activities also subsided the Sylhet Trough, presently at the rate of ~ 7–12 mm yr^{-1} (Reitz et al., 2015).

The stratigraphic framework of the Sylhet Trough (Figs. 1c and 2) was initially established lithostratigraphically to the type sections in the Assam Basin of the northeastern India (e.g., Evans, 1932; Shamsuddin and Abdullah, 1997; Khanam et al., 2021). Based on this correlation and recent sequence stratigraphic approach by Khanam et al. (2021), the stratigraphic units, from older to younger, of the Sylhet Trough are divided into three mega-sequence (Fig. 2).

3. Structure and tectonics

Except the western parts, all structural features framing the Sylhet Trough are the results of mostly the Pliocene-Recent compression along north, east and southeast (Hossain et al., 2020a). Moreover, stress orientation (Fig. 1a) related to plate boundary force varies around the Sylhet Trough (Kreemer et al., 2014; Heidbach et al., 2016; Yadav and Tiwari, 2018). Recent geodetic measurements suggest tectonic convergence with overall E-W and N–S shortening of this basin at ~7 mm yr^{-1} and ~18 mm yr^{-1} to the northern and eastern margins, respectively

Fig. 2. Summarized Cenozoic stratigraphy of the northeastern Sylhet Trough (after Reimann, 1993; Khanam et al., 2021). Except Tura Sandstone, all other formations are exposed and studied in this work.

(Nielsen et al., 2004; Steckler et al., 2016). This shortening produces anticlinal and synclinal structures as well as overlapping thrust systems verging to the south (in the northern part) and to the west (in the eastern part) within the Sylhet Trough. The fold system consists of a series of sub-parallel trending anticlines and synclines to the north and south-east, with respect to the Himalayan, and Indo-Burman orogenic trend, respectively. These two structural trends, with the geometry are dominantly controlled by pre-existing and concurrently developed reverse faulting, form a syntaxial pattern at the northeastern tip of the Sylhet Trough (Khan et al., 2018, 2019). The onset and later development of the sub-latitudinal trending fold system in the northern edge of the Sylhet Trough is basically controlled by the DFZ.

4. Data & methods

Structural measurements (attitude data) and deformation features were picked up from the eastern segment of the DFZ region (i.e., Jaintiapur area) in order to understand the surface geology, kinematics, and regional tectonics of the north-eastern edge of the Sylhet Trough, Bangladesh. We relate the outcrops-scale surface geology, bedding attitude, and kinematic data (fault-slip data, and geometry of the deformation structures) with the subsurface geology of the DFZ (Biswas et al., 2007a; Rosenkranz et al., 2018; Mallick et al., 2020) to determine the overall geometry and kinematics of the eastern segment of the DFZ.

To quantify the bedding geometry, the study area was divided into five segments/sections (Fig. 1d) based on surface geology and deformation patterns. Towards east these are *(a)* Dauki River-Mohammadi Chara section, *(b)* Tamabil-Naljuri-Sripur road cut section, *(c)* Nayagang-Kamalabari section, *(d)* Shari River section, and *(e)* Dupi Gaon section. Although the outcrops are sparsely exposed due to settlement, vegetation cover and rapid erosion, a geologic map of the study area was constructed in 1:25,000 scale (Fig. 1d). A geological cross-section (Fig. 1e) has also been constructed to illustrate the style of deformation in the subsurface. To do this, topographic profiles generated from *(i)* corrected 30 m Shuttle Radar Topography Mission (SRTM) topographic data, and *(ii)* the structural constraints picked up in this study from the Shari River section.

Bedding data for each studied segment was plotted using the Stereonet 11 software (Cardozo and Allmendinger, 2013). Fault-slip data (*n* = 12; fault plane attitude, amount of displacement, fault striae orientation, and sense of slip) were collected from the upstream (from the left bank in the Bet Ghat area) and downstream part (Putir Chara mouth) of the Shari River section of the study area (Appendix A). Common kinematic indicators including Riedel shears, shear bands, and bedding offset (~ 0.1–1 m) were used to determine the slip sense. Kinematic axes (incremental shortening, *P-axis*; and extension, *T-axis*) were estimated for each datum using the software FaultKin 8.1 (Marrett and Allmendinger, 1990). Principal shortening (σ_1) and extension axes (σ_3) for the total fault population in the study area were determined by calculating directional maxima for clusters of *P* and *T* axes following the Bingham statistics using the software FaultKin 8.1.

Kinematic interpretation of the outcrop-scale deformation structures was performed based on detailed field observations, oriented field photographs, geometric measurements of the bedding and structural features, and their overall relationship with the large-scale DFZ.

5. Results

5.1. Deformation structures & kinematics

Observations from field and satellite images in different scales suggest dominantly E-trending step-like thrust, and few ~ NNE-SSW oriented dextral-strike slip faults (Fig. 1d). Evidences of thrust (Figs. 3a–d, 5, 6, 7c, 8b, 9b), thrust duplex (Fig. 6a), fault breccia (Fig. 3b), fault striae (Figs. 7a and 8b), shear (Figs. 7b, 7f-g, 8a), transtensional fault (Fig. 4), seismites (Fig. 7d) and other brittle deformation features

(caption on next page)

Fig. 3. Deformation structures and stratigraphy in the DFZ at the Dauki River section near Ballaghat (inset map - Dauki-Mohammadi Segment: segment A in Fig. 1d). **(a)** 2D schematic diagram: thrust-shear planes, fault rock (breccia), unconformity (UC), and lithologic variation. Bedding and thrust-shear planes marked with black solid line, black dashed line, respectively. The uppermost unit represents poorly sorted gravels embedded in fine to coarse-grained matrix (recent deposit). Stereoplot at the lower right corner shows poles to the bedding (black), fault (red) and UC (blue) planes. Orthogonal thicknesses marked. Fault on the inset map delineated based on the present work. **(b)** Brecciated limestone along the brittle deformation zone indicating the DFZ. Fragments size ranges from tens of cm up to few mm. 15 cm long pencil as marker. The observed plane is sub-vertical. **(c)** Thrusted Sylhet Limestone and Kopili Shale along the DFZ. Field photograph broadly represents the schematic diagram (Fig. 3a). **(d)** Seemingly parallel minor thrust-shear plane (based on the presence of shear-sense indicator in the Kopili Shale as marked in Fig. 3f, ~20 m above), unconformity (UC) and bedding plane (S_0) are observed at the contact between the Sylhet Limestone and the Kopili Shale. The lower part of this limestone unit is fossil-bearing, whereas the upper part is mainly unfossiliferous with some m to cm-scale thin-bedded shale. **(e)** Kopili Formation (shale) unconformably overlies on top of the Sylhet Limestone. The contact (white line) represents an erosional surface (UC). Length of red Swiss-knife as marker is 10 cm (Photo is vertical). **(f)** Kopili Shale exhibits high fissility. The thickness of the limestone bed at the middle of the image is ~15 cm. The observed plane is sub-vertical.
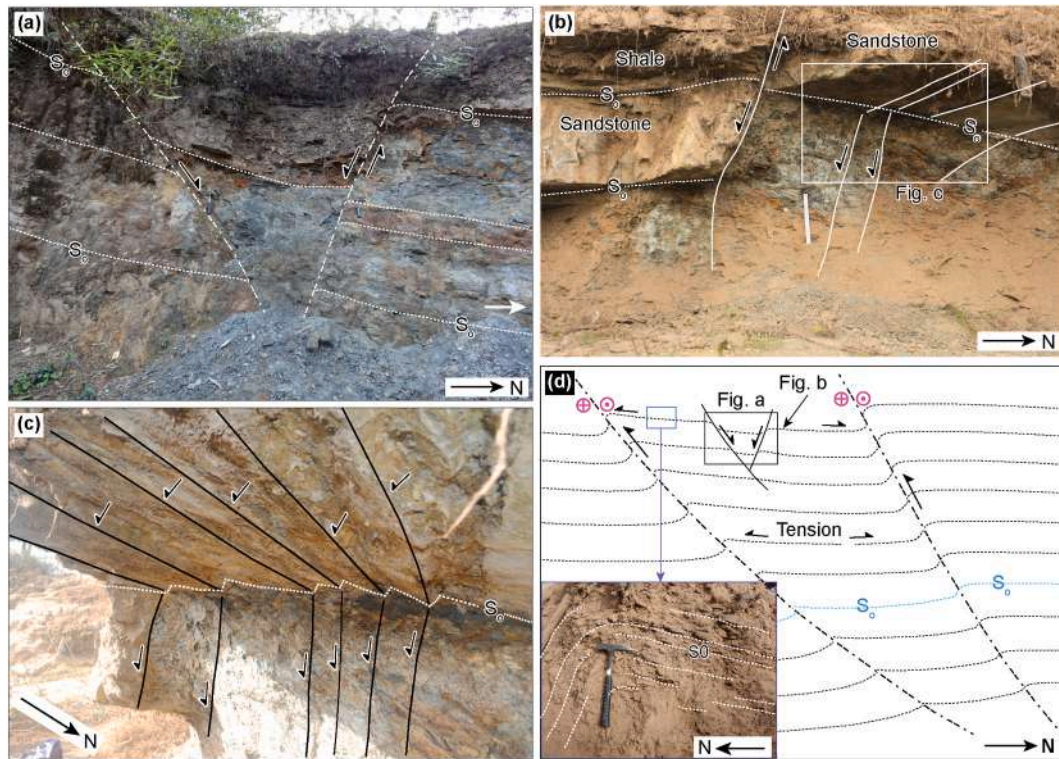
Fig. 4. Small-scale transtensional structures within contractional regime in the DFZ at the Tamabil road cut section (western part of the segment B in Fig. 1d). **(a)** A normal fault identified based on bedding (S_0, dotted white line) displacement and slip kinematics along the fault plane (broken white line) developed within the Barail Formation. White arrow: direction of the adjacent location fig. b. Length of hammer: 30 cm. **(b)** Fractured calcareous sandstone within Barail Formation. White dotted line: bedding (S_0), white solid line: fault plane. Scale length: 33 cm. **(c)** Cm to mm-scale en-echelon faults developed within calcareous sandstone. Black half arrows: slip sense. White dotted line: bedding (S_0). Snap length is ~1 m. **(d)** 2D transtensional model within contractional regime of the DFZ (location in inset map-Fig. 3a). Inset photograph shows thrust-induced drag folds. The main branch of the Dauki Fault is within ~500 m north of the area. Violet circles with cross and dot on both sides of the thrust fault mark the dextral kinematics.

(Figs. 3e, 7e and 9c) are present in all five segments of the study area.

In the westernmost part of the study area, in the Dauki River-Mohammadi Chara segment (segment A in Fig. 1d), both the relief and age of the exposed formations increase towards the north. The exposed Sylhet Limestone and Kopili Shale are highly deformed mostly in brittle manner due to their proximity to the DFZ (Fig. 3). Thick limestone breccias occur in the lowermost part of the Sylhet Limestone unit along the east bank of the Dauki River (Fig. 3a and b). Above it, ~ S-dipping bedded limestone shows thrust-shears with opposite vergence to that of the DFZ (Fig. 3a,c,d). The thrust planes parallel the bedding plane. A clearly visible thick erosional surface (138°/42°) between the Eocene Sylhet Limestone and Kopili Formation has been interpreted as a disconformity (Fig. 3c–e). The Kopili Formation appears to be sheared intensely by the DFZ (Fig. 3f). Around 5–20 cm thick limestone beds within the shale are also fragmented and slipped.

The deformation pattern of the exposed Barail Formation in the Tamabil-Naljuri-Sripur segment (segment B in Fig. 1d) varies much. In general, the deformation pattern shows more complexity in the western

part of this segment indicated by the variable dip directions (140–240°, few northward) as well as the dip amount (45–87°; Fig. 10b). Both transtensional and transpressional structures are observed in this segment. Interestingly, transtensional structures occur only in the western part (Fig. 4) as indicated by the presence of small-scale normal faults with ~0.1–1 m displacement. Well-developed en-echelon normal faults also exist (Fig. 4b and c). On the other hand, only transpressional/contractional deformation structures occur in the eastern part (Fig. 5). The thrusts are produced presumably by the sub-horizontal compression at the northern edge linked to the DFZ. In general, to the north and close to the DFZ, the thrust dips at a much higher angle (Fig. 5a), which gradually decreases towards south, and finally become sub-horizontal (Fig. 5b). A decrease in the degree of deformation in the direction of transport (owing to the formation of frontal thrust with low angle towards up-dip) and presence of the rigid Shillong Plateau as the hangingwall block are responsible for such a gradual variation of dip. The local thrust slices with similar vergence of the DFZ also occur here.

Deformation patterns of the exposed Bhuban Formation in the
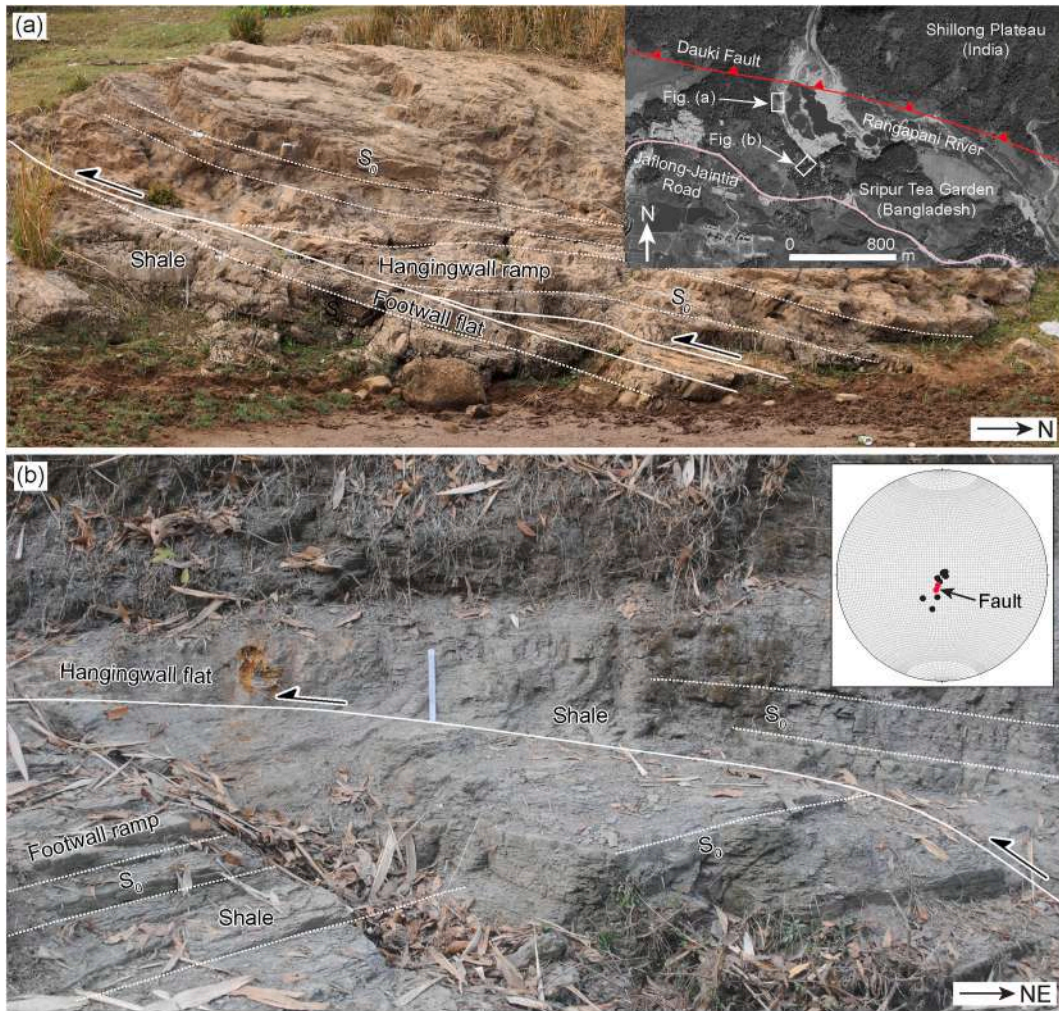
Fig. 5. Contractional structures within the DFZ at the Rangapani River section (inset map – central part of the Tamabil-Naljuri-Sripur Segment: segment B in Fig. 1d). Fault on the inset map delineated based on the present work. **(a)** South-verging thrusts within the shale show a kinematics similar to the DFZ. White dotted line: bedding (S_0), white solid line: fault plane. Snap length ~20 m. **(b)** Approximately south-verging low-angle thrust fault (i.e., overthrust) developed with the shale (Barail Formation). The exposure is located ~500 m south of the exposure in figure (a). Half arrow: slip of hanging wall. White dotted line: bedding (S_0), white solid line: fault plane. Stereoplot at top right: poles of bedding (black), and fault (red). Scale length: 33 cm.

Fig. 6. Thrusting of the shale unit (Bhuban Formation) exposed along the Kamalabari-Gaurishankar road cut section (inset map – Part of Nayagang-Kamalabari segment: segment C in Fig. 1d). Fault on the inset map delineated based on the present work. **(a)** An approximately south-dipping thrust duplex developed in shale. White dotted line: S_0 bedding; white solid line: thrust plane. Marked scale length on the snap is 33 cm. **(b)** Zoom of the rectangular part of the fig. (a)- S_0 is discordant across the thrust. Inset stereoplot: poles to the bedding (black), and fault (red) planes. Scale length: 33 cm.

Nayagang-Kamalabari section (segment C in Fig. 1d) suggest that this area is deformed less than the western two segments. A major unconformity marks the contact between the Oligocene Barail Group and the Miocene Bhuban Formation at the western edge of the Nayagang-Kamalabari segment. Immediately above the contact, south-verging small-scale parasitic folds, possibly thrust-induced, occur in the Bhuban Formation. In this segment, the bed dips uniformly to the south with few exceptions related to local thrusting. Thrust duplex with metre-scale
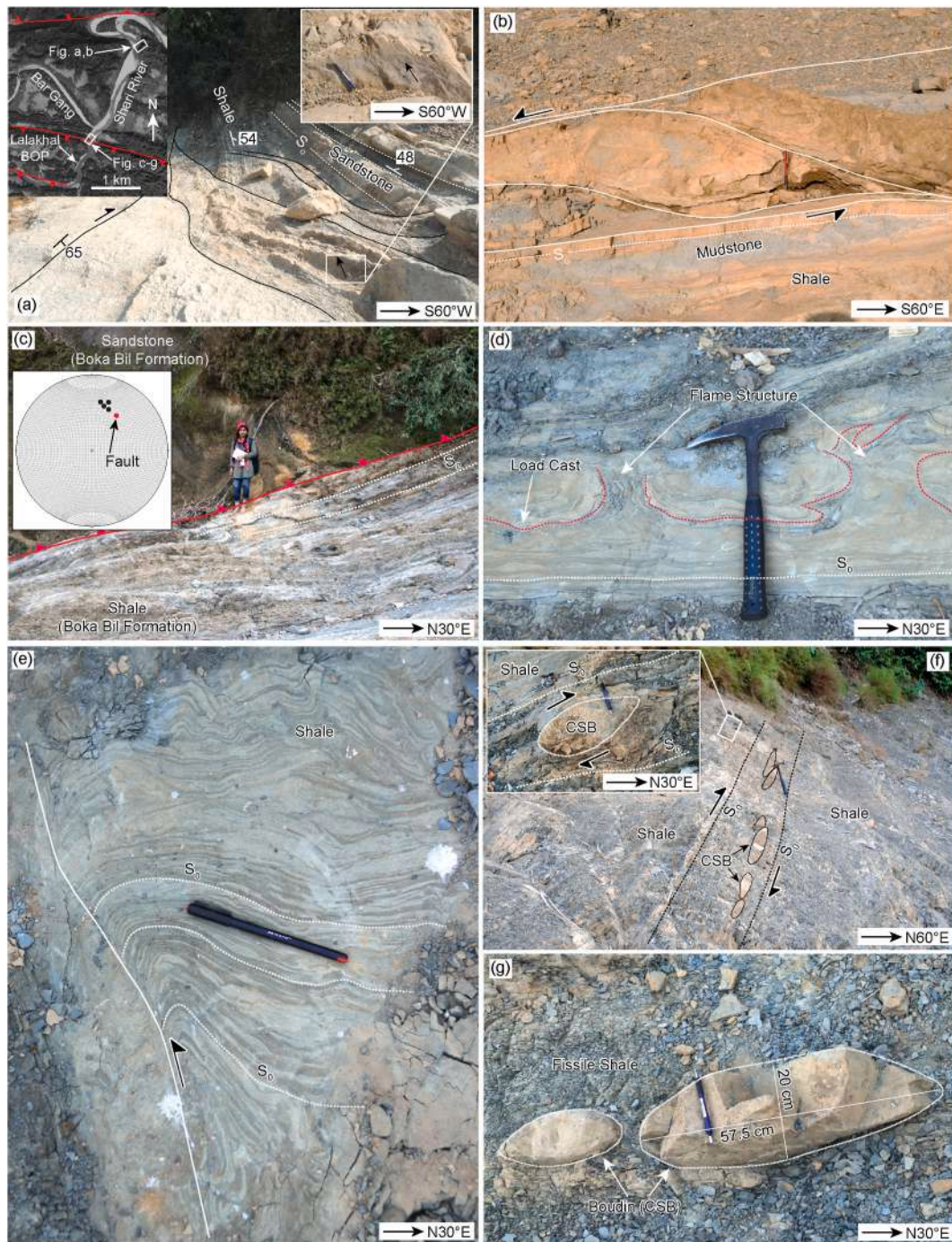
Fig. 7. Contractional structures in the Shari River section (segment D in Fig. 1d) east of the Lalakhal Border Guard Post (BGP) (inset map - upstream part of the Shari River Segment). Fault on the inset map delineated in this work. **(a)** Thrusts developed in the shale unit (Boka Bil Formation) along the Shari River section near Bet Ghat. Approximate length of the snap is 10 m. Black arrow in the zoom picture marked the striation line suggesting the direction of hanging wall movement. Length of pencil as marker: 15 cm. **(b)** Sigmoid structure with sinistral kinematics developed in the shale unit (Boka Bil Formation) near Bag Chara. Length of pencil as marker: 15 cm. **(c)** Fault in the upper part of the Boka Bil Formation that separates upper sandstone unit from lower shale unit. The fault is a thrust with northward vergence. Mini Saha as marker, 1.55 m height. **(d)** Seismites (flame structure) formed in the shale unit, immediately below the thrust-contact of the Tipam and Boka Bil Formation. Length of hammer as marker: 0.30 m. **(e)** Small-scale brittle-shear structure in which shale layer subjected to mainly brittle deformation to the left and dominantly ductile deformation on the top right. Shear sense (black half arrows) assigned considering the folded layer to be a normal drag (review in Mukherjee 2014). Length of pen as marker: 15 cm. **(f)** Dextral sheared shearband boudins consistent with adjacent thrust plane kinematics. The competent rock of the Shearband boudin is the Calcareous Sandstone Band (CSB). Length of hammer as marker: 0.30 m. CSB in the zoom picture shows the shear band boudin. Length of pencil as marker: 15 cm. **(g)** Phacoidal boudins, developed in the competent Calcareous Sandstone Band (CSB). Length of pencil as marker: 15 cm.

displacement locally shows opposite vergence to that of the DFZ (Fig. 6). The attitude of the thrust plane is approximately 45°/155°. Thrust imbricates link the floor thrust to the roof thrust of the duplex (Fig. 6a). These kinds of thrusts with commonly sigmoid P-planes are known as the link thrusts (McClay and Insley, 1986). As the exposures are discontinuous, often covered by vegetation and settlement, and mostly unconformably overlain by a boulder bed (Dihing Formation), it was difficult to document other structures.
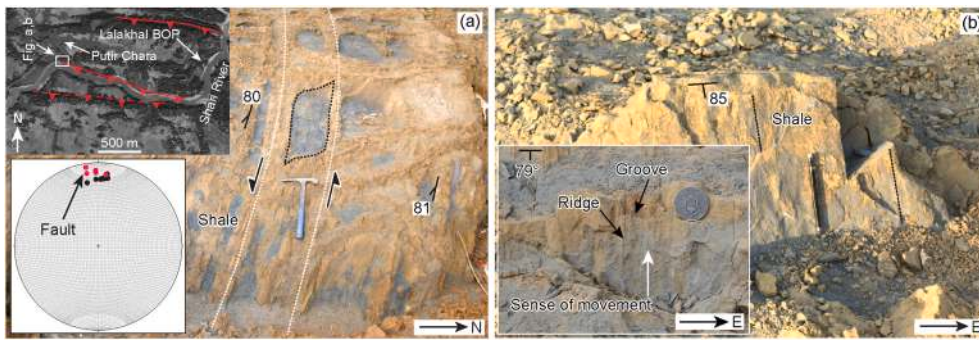
Fig. 8. Evidence of contractional deformation structures (thrust-shear zone) in the Shari River section (segment D in Fig. 1d) at the mouth of Putir Chara (inset map - downstream part of the Shari River Segment). Fault on the inset map delineated based on the present work. **(a)** Shale (Boka Bil Formation), which is thrust on top of the sandstone (Tipam Formation) shows sigmoid structures due to ductile deformation. Length of hammer as marker: 0.30 m. Stereoplot at the lower left corner shows poles to the bedding (black), and fault (red) planes. **(b)** Well-developed striation on a thrust plane. Black dotted lines: striae. The striation trend and plunge are ~163° and 78°, respectively. Length of pencil as marker: 15 cm. Inset photograph shows the sense of thrust movement (white arrow) based on slickenside with groove and ridge.
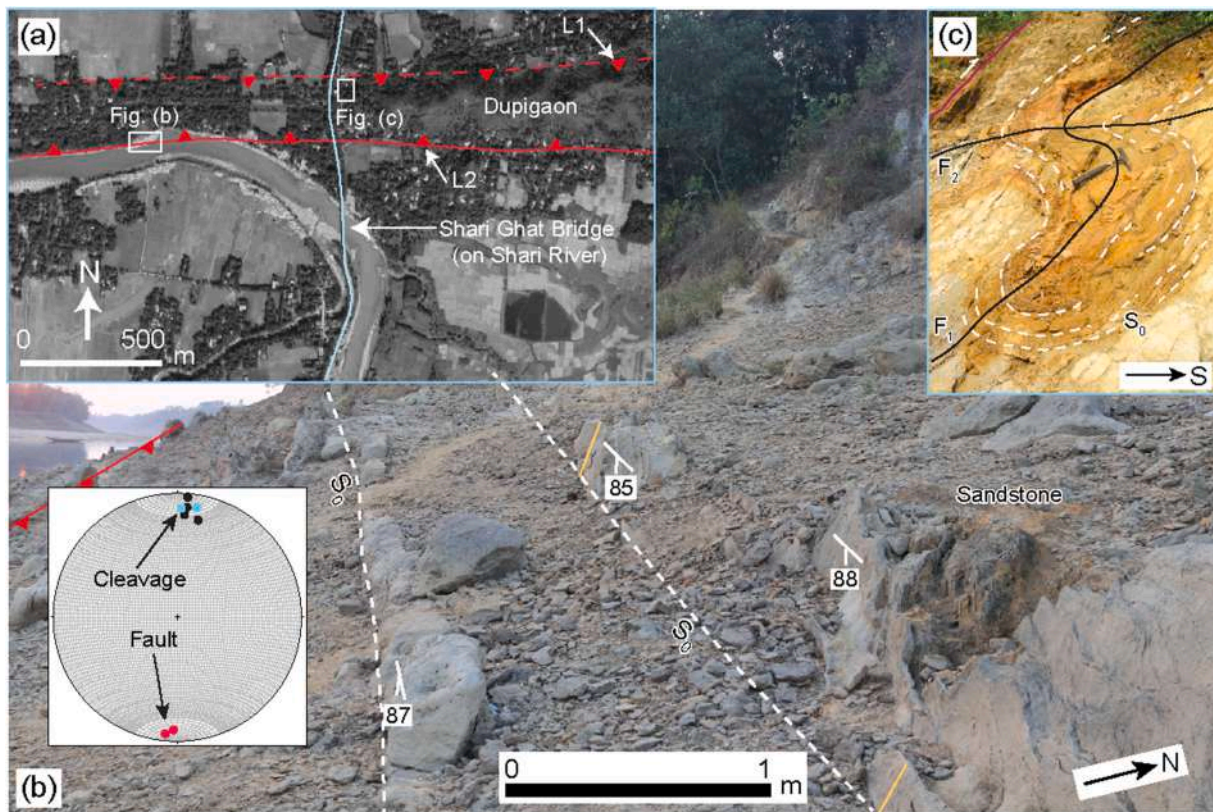
Fig. 9. Thrust-shear deformation observed within the Dupi Tila Formation exposed along the Shari River segment (segment E in Fig. 1d) near the Shari Ghat Bridge (inset map – west part of the Dupi Gaon Segment). Fault on the inset map delineated in this work. **(a)** Panchromatic satellite image taken from the Google Earth Pro and its interpretation showing the Dupi Gaon Hills (type section of the Dupi Tila Formation) developed geologically as a possible pop-up structure. Solid and dashed red lines indicate confirmed and possible thrusts, respectively. **(b)** Near-vertical sandstone (Dupi Tila Formation) crops out along the river bank. Golden-yellow line: dragged bedding planes, S_0: the bedding plane. Stereoplot at lower left: poles to the bedding (black), fault (red) and cleavage (blue) planes. (c) Local parasitic fold developed due thrusting. The first generation folding (F_1) is mainly related to thrusting (Fig. 9a) and the second generation of folding (F_2) is related to the overall dextral transpression. Red line (top left): local shear plane, white dashed lines: S_0 bedding, solid black lines: two generations of local fold's axes (F_1, and F_2). Length of hammer as marker: 0.30 m.

Several transpressional/contractional structures (Figs. 7 and 8) are identified in the exposed rocks of the Shari river segments (segment D in Fig. 1d). Towards south, the exposed rocks in these segments are Boka Bil, Tipam and Girujan Clay formations (Fig. 1). Here the path of the Shari River is mainly fault-controlled (Fig. 11a). The inference of structural control Shari River course is primarily based on the straight courses of the river immediately on the foothills with an abrupt slope difference, and the repeated straight courses with sharp bending in between. This inference is manifested by dip direction reversal and abrupt change of dip amount (Fig. 1d), repetition of the older strata along the

down-dip direction (Fig. 1d), and other deformation features exposed along the river bank (Figs. 7–9). Five faults are identified in the Shari River segment, out of which three faults trend E-W, and the remainder trends ~ NNE (Fig. 11a). The former three faults are mainly dip-slip (thrust/reverse) and the others are mainly strike-slip (dextral) in nature. In the upstream part of the Shari River, strong deformation contrast is observed between thinly bedded, and internally folded and faulted sandy shale unit, and thickly bedded almost undeformed sandstone unit of the Boka Bil Formation possibly due to competence contrast (Fig. 7a). Locally, fault outcrop shows thrusting with visible slip. Thrust
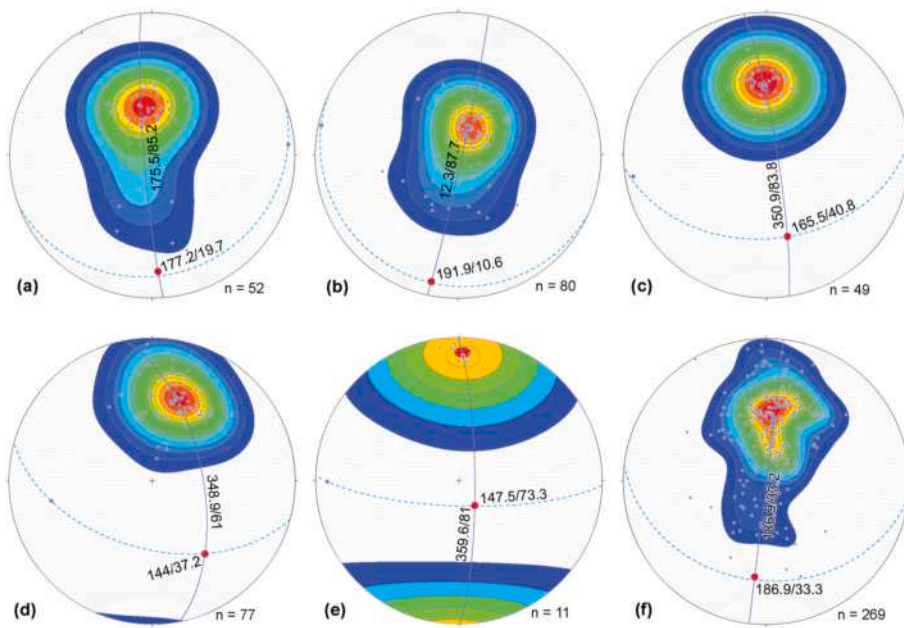
Fig. 10. Stereograms show poles to bedding (blue points) with a cylindrical best fit line (magenta solid line) and pi axis (red circle) for each segment as well as for whole study area. The orientations of the bedding attitude data for each studied segment was determined using a cylindrical best fit to poles to bedding using the Stereonet 11 software (Cardozo and Allmendinger, 2013). Bedding to mean pole (blue dash) follows Right Hand Rule (RHR). All stereograms are equal area lower hemisphere projections (Cardozo and Allmendinger, 2013). **(a)** Dauki River-Mohammadi Chara segment (segment A in Fig. 1d), **(b)** Tamabil-Naljuri-Sripur road cut segment (segment B in Fig. 1d), (c) Nayagang-Kamalabari segment (segment C in Fig. 1d), (d) Shari River segment (segment D in Fig. 1d), **(e)** Dupi Gaon segment (segment E in Fig. 1d), and **(f)** combined datasets of all these sections. The orientation of the pi axis (hollow red circle) is labelled with trend and plunge. Note n: number of bedding attitude data.
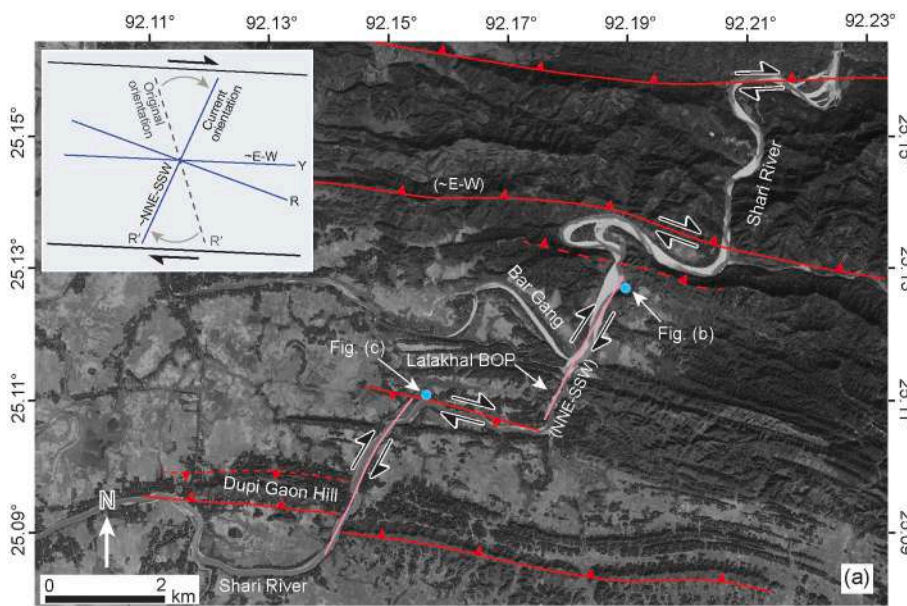
Fig. 11. Faults in the Shari River segment (segment D in Fig. 1d) and their slip-mechanism. **(a)** Geo-referenced background panchromatic satellite image taken from the Google Earth Pro. Faults marked on the map are picked up by fieldwork during this study. Inset schematic diagram is the dextral Riedel shear model of the eastern segment of the DFZ and the associated local faults. **(b)** Equal area stereograms with fault-slip data are shown for the Shari River section (upstream part in the Boka Bil Formation). Black great circles: fault planes; black arrows: slip lineation and motion of the hanging wall. Red and blue circles: incremental extension (T) and shortening axes (P), respectively for each fault (following Marrett and Allmendinger, 1990). The average maximum and minimum principal axes of infinitesimal strain from fault slip analysis are indicated by σ₁ and σ₃, respectively (σ₁ – maximum, σ₂ – intermediate, and σ₃ – minimum). Note n: total number of fault plane data. (c) Fault plane solution in the Putir Chara area of the downstream part of the Shari Rivers section (from the right bank and in the Boka Bil Formation).
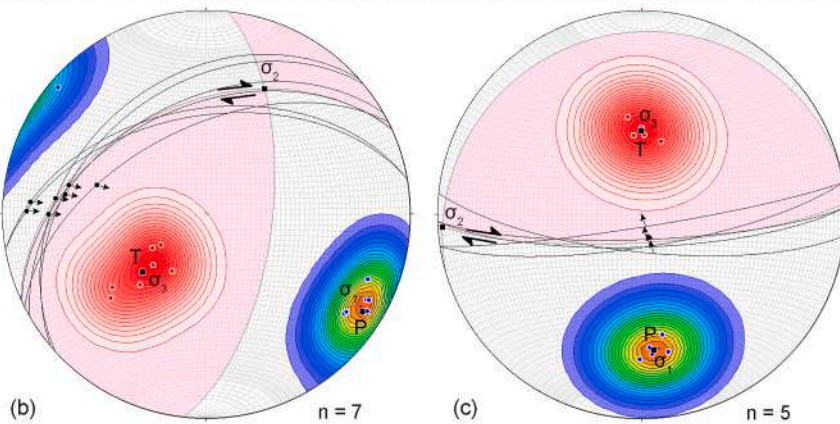
kinematics suggests ~ NNW-dipping thrust with the dextral strike-slip component responsible for both brittle and ductile deformations. Although the overall deformation pattern suggests a dextral kinematics, locally opposite kinematic vergence (i.e., sinistral shear; Fig. 7b) is also present (Dutta and Mukherjee 2019).

Approximately 2.5 km downstream of the Shari River (segment D in Fig. 1d; near the mouth of the Bar Gang), the transition between BokaBil and Tipam formations has been observed (Fig. 7c). Deformation localization at the lithological interfaces is a known phenomenon (e.g., Mulchrone and Mukherjee 2015). Immediate below this transitional contact, thinly bedded sandy shale unit is intensely brittle-ductile deformed (i.e., sheared; Fig. 7f). The presence of flame structure (seismites) related to seismically-induced liquefaction or fluidization (Fig. 7d), small-scale thrust (Fig. 7e), and asymmetric shearband boudins with dextral shear (Fig. 7f) confirm the presence of fault. The competent Calcareous Sandstone Band (CSB), common in the Boka Bil Formation, separate into pieces through brittle-plastic deformation and form phacoidal structure (Fig. 7g). All these thrust-shear related kinematics are similar to that of the DFZ kinematics, immediate north of this area.

Further downstream, at the mouth of the Putir Chara (segment D in Fig. 1d), stratigraphic repetition has been observed. In the down-dip direction, although repetition of the older formation (Boka Bil) on top of the younger formation (Tipam) noted in sub-vertical sections (Fig. 1d and e) and sharp increase of the dip amount suggest reverse faulting, shear fabric (Fig. 8a) in the mudstone embedded in the sandy shale unit (Boka Bil Formation) suggest also the presence lateral-slip/shear component of the fault. Striations-bearing thrust planes dip ~ south (Fig. 8b). The vergence of the thrust is similar to the regional Dauki Fault.

The Dupi Gaon segment (segment E in Fig. 1d) belongs to the southernmost part of the study area, i.e., in the down-dip direction, and therefore, the exposed Dupi Tila Formation is the youngest rock formation in the area. This formation experienced the last episode of the Himalayan orogeny and is derived mainly from recycled felsic source (Rahman et al., 2020). Satellite images show that the eastern part of the Dupi Gaon/Tila Hills are offset laterally across the ~NNE oriented Shari River segment (Fig. 11a). Kinematic interpretation of the offset ridges of the Dupi Gaon Hills suggests a dextral-slip. Two E-W oriented lineaments (L1 and L2) that are ~ 12 km long are distinct in the satellite images at the northern and southern edge of the Dupi Tila Hills (Figs. 9a and 11a). Field observations suggest that these lineaments are basically thrusts (Fig. 9b and c). Approximately 500 m downstream from the Shari Ghat, field evidences of reverse faulting are clearly visible along the southern lineament (Fig. 9b). Sub-vertical bed and bedding offset suggest ~ SSE-verging thrust with strike-slip components. Along the northern lineament, near-vertical dip was also observed during the fieldwork.

5.2. Results of bedding geometry analysis

Bedding patterns (total data points, $n = 269$) collected from five segments (Fig. 1d with marked segments) show consistent E-W strike with variable dip with a predominantly southward dip direction. Although beds in the Dauki River-Mohammadi Chara segment (Fig. 10a), and the Tamabil-Naljuri-Sripur segment (Fig. 10b) show similar attitude patterns, dips vary more in the latter segment. Rather than predominantly dipping to the south, quite a number of beds show northward dip in the Tamabil-Naljuri-Sripur segment. The trend and plunge of the fold axis in the Dauki River-Mohammadi Chara segment and the Tamabil-Naljuri-Sripur segment are 177.2°/19.7°, and 191.9°/10.6°, respectively. In general, beds dipping to the north have lower angle than the south-dipping beds. The western portion of the Tamabil-Naljuri-Sripur segment shows reverse dipping beds (i.e., dipping to the north) of the Barail Formation and apparently suggests local anticline. The sub-horizontal fold axes trend ~282°, and the interlimb angle is

~142°. In these two segments (Dauki River-Mohammadi Chara, and Tamabil-Naljuri-Sripur segments) (Fig. 1d), brittle deformation structures (faults, joints and cleavages) are more dominant than in the other segments. The cleavages are related to secondary shear plane developed in transpressional thrust-shear zone. Both transpressional (thrust fault – Fig. 3a–c, 5) and transtensional (normal fault – Fig. 4) deformations are observed.

Bedding in the Nayagang-Kamalabari, and the Shari River segments (segments C and D, respectively in Fig. 1d) show consistent dip to the south. Dense pole plots of these two segments in the stereonet (Fig. 10c and d) indicate that these areas are tectonically less disturbed and opposite dip directions have not been observed in these areas. The trend and the plunge of the axis in the Nayagang-Kamalabari segment and the Shari River segment are ~255°/9°, and ~144°/37°, respectively. However, compared to the western Dauki River-Mohammadi Chara and Tamabil-Naljuri-Sripur segments (segments A and B, respectively in Fig. 1d), dip amounts of the bed increase in these two portions (Fig. 10c and d). Dip of the bed for the Nayagang-Kamalabari and Shari River segments are 41 and ~51°, respectively. The only visible difference observed between the Nayagang-Kamalabari and Shari River segments is the slight deviation of the dip direction orientation with respect to the south. In the Nayagang-Kamalabari segment, the dip direction of the bed is slightly deviated to the east from south (~175°), whereas in the Shari River segment, the dip direction of the bed deviated to the west from south (~196°). In these two segments, brittle (fault, joint), and brittle-ductile (boudins, shear bands) deformations are observed. Only the transpressional deformation (thrust fault – Fig. 6) is observed in these parts of the study area.

Bedding in the Dupi Gaon segment (segment E in Fig. 1d) shows consistent dip (45–88°) to the south. The trend and plunge of the axis in this segment are ~148° and ~73°, respectively. However, compared to the other four segments, dip of the bed are significantly higher (Fig. 10e). Beds are significantly disturbed by minor faulting and folding, and bedding parallel cleavage (Fig. 9b). The meter-scale plunging to non-plunging, asymmetric, and sub-horizontal folds are developed within sub-vertical beds in the Dupi Gaon section (Fig. 10). The mean dip direction and dip amount in this segment are ~182°, and ~76°, respectively. Combined results of the five segments suggest that the trend and plunge of the monoclinal axis is ~187°/33°. In the entire study area, the overall dip direction and dip amount of the beds are ~187°, and ~31°, respectively.

5.3. Fault slip analysis results

Although a number kinematic indicator (Riedel shears, shear bands, slickensides, and offset bedding) of the faults is available in all the segments of the study area, exposed clean fault surfaces are rare since the soft sedimentary rocks are much eroded. Slickensides and bedding offset were mainly used to determine the slip sense. Analysis was performed based on the fault attitude, striae trend and plunge, and sense of slip measurements (Appendix A). In the upstream area of the Shari River segment (Location in Fig. 11a), the results of the fault slip analysis suggest the trend and plunge of the P and T axes value of the fault plane are 122°, ~11°, ~228° and ~55°, respectively. The strike, dip direction and dip amount of the fault plane is 246°, 336°, and 45°, respectively. This suggests a dominantly dip-slip thrusting (Fig. 11b). In the downstream area (Putir Chara; location shown in Fig. 11a), the result of the fault plane solution suggest the trend and plunge of the P and T axes value of the fault plane are ~178°, 34° and 360°, 56°, respectively. The strike, dip direction and dip amount of the fault plane is ~087°, 177°, 79°, respectively. The result of this second fault slip analysis suggests dip-slip (thrust) fault (Fig. 11c). The fault kinematic analysis of the upstream part of the Shari River indicates horizontal shortening subparallel to the east-west oriented DFZ (Fig. 11b), whereas, in the downstream part (Putir Chara), subhorizontal shortening ~ perpendicular to the east-west oriented DFZ (Fig. 11c) has been observed. The

result of the fault slip analysis (Fig. 11b and c) suggests that none of the principal stress axes are horizontal and that means the study area is subjected to a non-Andersonian stress regime.

6. Discussions

The investigated area forms an east-west narrow strip at the eastern side of the ~320 km long DFZ (e.g., Bilham and England, 2001; Hossain et al., 2019). Structurally, the area is situated within the footwall of the DFZ (Fig. 1a), north of the Khawi and Kushiara synclines and Gowainghat anticline (Hossain et al., 2020c). In general, elevation gradually decreases towards the south with the exception of the E-W trending linear ridges and piedmont plains (Fig. 11a). This suggests the stronger forces acted towards the north along the DFZ during the formation of the hillocks (Chowdhury et al., 1996). Approximately NNE-SSW and EW straight courses of the major rivers (Fig. 1c) are anticipated to be the result of linear structural features (thrust, strike-slip) developed sympathetic to the major stress field in the area. According to Khan et al. (2006) and Monsur (2020), the matrix-supported gravel beds, which cap few hill tops might be alluvial fan deposits of the palaeo-drainage systems and marks few small terraces in the area (Khan et al., 2006; Monsur, 2020). The ages and thicknesses of the gravel beds around the Dauki River and the Kamalabari sections indicate spatial and temporal differences in their deposition and recent uplift (Khan et al., 2006).

6.1. Interpretation of the bedding attitudes

Analysis of the bedding measurements in the five segments shows predominantly south-dipping strata with variable dip amounts (Fig. 10). Poles to bedding from the five segments form generally north–south-striking girdles, cylindrical best fits to the data indicate subhorizontal east–west-trending antiform fold axis for the structure, which gently plunges to the west. Therefore, geometrically the area can be interpreted as a large-scale monocline, consistent with the previous interpretation (Biswas and Grasemann, 2005b; Biswas et al., 2007b; Chowdhury et al., 1996). Our results also suggest that the trend and plunge of the monoclinal pi-axis are ~187°, and ~33°, respectively. The area is subjected to mainly ~ N–S compression, however, ~E-W stress field are also observed to the eastern edge of the Sylhet Trough related to westward propagation of the Indo-Burman Wedge (Fig. 1a) (Mallick et al., 2020). Therefore, the overall trend of the monoclinal structure reflects the tectonics of the area. However, opposite dipping (i.e., dipping to the north) are also observed in the Dauki River-Mohammadi Chara segment, and Tamabil-Naljuri-Sripur segment (Fig. 10a and b). These areas are tectonically more disturbed due to high compressional forces and strain portioning along the DFZ. Although the western portion of the Tamabil-Naljuri-Sripur segment (Fig. 1d –Tama Bil area) shows several oppositely dipping bedding planes and apparently suggests anticline but it is more possibly due to roll-over against the Dauki Fault (Chowdhury et al., 1996). This roll-over anticline is possibly related to the reverse drag of the footwall against the Dauki Fault (Brandes and Tanner, 2014), and could be a good hydrocarbon trap (Fig. 13d).

Compared to the western two segments (Fig. 10a and b) dip of the bed increases in the three eastern segments of the study area (Fig. 10c–e). Monoclinal structures, in general, show higher dip in the older formations and lower dip in the younger formations. Chowdhury et al. (1996) reported similar observation while working along the Shari River segment. However, during field investigation from the upstream (Older formation – Boka Bil) to downstream (Younger formation – Dupi Tila) of the Shari River segment, the absence of such decreasing dipping trend in the down-dip direction (Fig. 1) suggest that the area is tectonically disturbed/faulted. In general, a clock-wise switching (~35°) of the mean bedding dip direction from the Dauki River-Mohammadi Chara segment (~159° - based on fieldwork) on the west and to the Shari River segment (196°) on the east (Fig. 10) essentially denote the trend of the

DFZ adjacent to these segments (Fig. 1b). Comparatively higher order of strike deviation, nearly opposite dip direction, and dominance of other brittle shear-structures in the western half of the Tamabil-Naljuri-Sripur segment are therefore interpreted to be associated with the clear clock-wise bending of the Dauki Fault immediate north of this segment (Fig. 1d; near 92° 05′ longitudinal marking).

6.2. Interpretation of the fault slip analysis

Tectonic stress regime of an area can be analysed through fault slip analysis (Misra et al., 2014; Vanik et al., 2018; Dutta et al., 2019; Mukherjee, 2019; Shaikh et al., 2020; Maurya et al., 2021). In the present study, analyses have been performed in two locations of the Shari River segment (segment D in Fig. 1d). In the upstream area of the Shari River segment, the kinematics revealed from the fault plane solution (Fig. 11b) suggests a right-lateral slip. Based on focal mechanisms for the different hypothetical fault systems, the current result suggests mostly a dip-slip motion with some strike-slip component having dextral wrenching (Stein and Wysession, 2003). The river course at this location is slightly offset by the fault striking ~246°. In the downstream area of the Shari River segment, the kinematics revealed from the fault plane solution (Fig. 11c) and its comparison to the focal mechanisms for different hypothetical fault systems (Stein and Wysession, 2003) suggests mainly a dip-slip thrusting. The fault is ~ sub-parallel to the river course (087°N) here. Although faults in these two locations show different geometric attributes and their fault plane solutions show different kinematics, both of them should be related to the ESE-WNW and NNE-SSW major principal stress (σ_1) regime (Fig. 1a) that can be considered responsible for the overall deformation of the DFZ in this area. The small inconsistency in the fault trend data (228–260°: Shari River upstream, and 81–96°: Shari River downstream/Putir Chara) reduces considerably after fault slip analysis (upstream faults - ~246°; downstream faults- ~087°), generating maxima and sub-maxima along certain orientations that are consistent with the study area.

Therefore, it is envisaged that all the faults in the region have suffered the same deformation as that of the DFZ. Although fault slip-analysis in the two locations reveals right-lateral (Fig. 11) deformation, structures with sinistral kinematics are found in both the locations (Figs. 8b and 9a). This phenomenon can be explained through the Riedel shear system (Swanson, 1988), where most of these fault orientations coincide with the primary R (right-lateral), P (right-lateral), R' (left-lateral), and T shears of a dextral Riedel shear system (inset diagram in Fig. 11a). The overall kinematic analysis of faults indicates a sub-horizontal shortening along NNW or NW, which is at a high-angle to the east-west oriented DFZ. Incremental strain axes determined from fault-slip analyses indicate a bulk north-trending sub-horizontal shortening and the compressed layer subjected to vertical thickening. Hence, the fold and fault developed within these layers are also subjected to vertical thickening.

Altogether, map patterns of the bedding dip distributions, stereographic analysis of the attitude data, and fault-slip analysis indicate that monocline and faults in the southern edge of the Shillong plateau accommodate plane strain with generally north–south-trending, sub-horizontal shortening axis (maximum principal stress axis, σ_1; Fig. 11) that are almost orthogonal to the axial trace of the monocline (Fig. 10f).

6.3. Synthesis of the deformation structures kinematics

Structural synthesis performed in this study is mainly based on the field kinematics of the observed deformation structures and their relation with the DFZ. The presence of S-vergent fault in the Nayagang section (Fig. 5), N-verging and S-dipping bedding-parallel shear in the Dauki River (Fig. 3a,c) and the Kamalabari-Gaurishankar sections (Fig. 6) indicate a northward sub-horizontal shortening (maximum principal stress, σ_1) of the monoclinal fold as also suggested by the fault slip analyses (Fig. 11b and c). Flame structure observed in the Miocene

Boka Bil Formation in the Shari River section can be seismicity-induced (Meghraoui and Atakan, 2014). We infer so since the structure is within the DFZ. Palaeoseismic events related to DFZ have also been reported adjacent to this study area (Morino et al., 2011, 2014). Modern geodetic velocity field measurement also suggests seismicity along the DFZ in recent past (Mallick et al., 2020).

Boudins of the calcareous sandstone band occur in the Miocene Boka Bil Formation and their geometry (Fig. 7g) suggests the brittle-ductile (plastic) deformation with a dextral slip. The aspect ratios (long axis divided by short axis) of the CSB boudins in the Shari River section ranges 2–4. Boudinage normally results from the stretching of a competent but flexible stratum (here it is CSB) during the slip (Goscombe et al., 2004). Although the monoclonal fold is generally related to the reverse fault-propagation (Erslev, 1991) as in the case of the current study area (Chowdhury et al., 1996), the presence of pha-coidal boudin, S-vergence, and approximately north-verging faults also suggest the existence of slip or flexure-slip mechanism. Further, while the majority of the kinematics data suggest a dextral-slip, few sinistral faults also exist (Figs. 7b and 8a). The presence of such opposite shear sense (OSS) is reported in different tectonic terrains (Dutta and Mukherjee, 2019). OSS can develop due to orthogonal switching of the principal stress axes or tectonic inversion in sedimentary basins. Orthogonal switch is likely due to east-west compression along the Chittagong-Tripura Fold Belt (CTFB). In addition, the OSS phenomenon can also possibly be explained through Riedel shear system (Swanson, 1988), where most of these orientations coincide with the primary R (right-lateral), Y (right-lateral), and R' (left-lateral) of a dextral Riedel shear system.

Local faults observed in different segments of the study area are most likely produced concomitantly as well as later due to strain partitioning of the DFZ. With respect to the regional dextral DFZ (Lindsey et al., 2018; Panda et al., 2018; Hossain et al., 2020c), approximately E-W orientated local faults (Figs. 1d, 6 and 7a, 8, 9, 11a) matches with the synthetic Y, and R of the dextral Riedel shear structure (inset map: Fig. 11a). However, the NNE-SSW-oriented faults (Fig. 11a) do not correlate with the dextral Riedel shear model with respect to DFZ. This mismatch is possibly related to successive complex evolution of the DFZ (Fig. 13) since its inception in the latest Miocene up to the earliest Pliocene (Govin et al., 2018). With progressive strain, the initial anti-thetic faults currently orient sub-parallel to shear direction due to intense clockwise rotation within the DFZ domains. Such rotation of the Riedel shear structures are well documented in the literature (Katz et al., 2004).

The principal strain (shortening) axis at the northwestern edge of the Sylhet Trough (just on the DFZ) is NE-SW, whereas, in the southeastern edge of the trough, and the principal strain (shortening) axis is ENE-WSW (see Fig. 7e in Kreemer et al., 2014). This clockwise rotation of the strain axis to the east of the Sylhet Trough is related to the westward propagation of the Indo-Mayanmar Ranges in this area. The strain axis alignment matches with the orientation of the maximum horizontal compressive stress of the area (Fig. 11a; Heidbach et al., 2016; Yadav and Tiwari, 2018). In addition, the GPS-derived velocity field mea-surement also suggests ∼ NE movement of the northeastern part (Sylhet Trough and adjacent region) of the Indian Plate (Mallick et al., 2019). The principal stress axes orientation determined from the fault slip analysis (Fig. 11b and c) in this study is accorded the prevailing strain axis, stress field, and GPS-derived geodetic measurement of the study area.

Near-parallel faults in the Dauki Fault zone bound 10–15 km long ∼ E-W trending ridges (Fig. 11a), which record different degrees of tilting as suggested by variable dip amount of each fault at the different faults-controlled ridges. As a result, both dextral and sinistral wrenching is observed locally, specifically along the Shari River segment (Figs. 1, 7 and 8l a). Depending on the straight course and clear bending, the Shari River can be divided into five segments. Two segments with ∼NNE/N-SSW/S trend have been identified as lineaments (Biswas and

Grasemann, 2005a). Field observations (fault-slip data – Fig. 11b and c; shear sense indicator – Figs. 7 and 8) and clear offset of the Dupi Gaon Hill along the down-stream segment (Fig. 11a) clearly suggest mainly dextral wrenching with a dip slip-component (Fig. 11). On the other hand, stratigraphic repetitions, bedding offset, steep dip and other deformation kinematics suggest three ∼ E-W segments that are mainly thrust-controlled with dextral-slip components (Fig. 11b). Presence of meter-scale, plunging to non-plunging, asymmetric and sub-horizontal folds within sub-vertical beds at the northern and southern edge of the Dupi Gaon section suggests fault-controlled pop-up structure (Fig. 9). The sub-vertical bedding at the southern edge of the Dupi Gaon Hill along the northern bank of the Shari River is related to compressional upthrusting of the sandstone along thrust fault (Fig. 9). Linear ridge-like features of the study area show conspicuous 'kink' type geometry in the DEM (Fig. 11a; also see the Main Map of Hossain et al., 2020c). The exposed Bhuban to Dupi Tila Formation are compositionally uniform and dip to the south (Chowdhury et al., 1996), Biswas and Grasemann (2005a) assumed that the observed geometric effect of the monoclinal fold with several linear ridges is the result of erosion along bedding parallel fractures. However, during the field investigation, we observed evidences of dip-slip and strike-slip kinematic features along few of these fractures (Figs. 6–8, 11). Presence of monoclinal fold, local roll-over anticlines, fault-bounded anticlines and transverse faults in this proven petroleum system suggest that these structures can likely act as possible hydrocarbon traps.

Tectonically, the DFZ has a complex spatial and temporal evolution (Biswas and Grasemann, 2005a). The Dauki Fault, its main structure, is not a single fault but constitutes a fault zone (outcrop-level thickness: ∼ 5–6 km, orthogonal thickness: ∼3.89 km). According to Hiller and Elahi (1984), a major branch of the Dauki Fault verges to the south and goes below the alluvium at south of Atgram of the Sylhet Trough (Bangladesh) as a blind ∼ E-W trending thrust. The Dauki Fault and this kinematically-related blind thrust to the south deformed the Tertiary sediments into a large-scale monocline (Biswas and Grasemann, 2005a, b). Perturbation strain caused by these two faults variably uplifted the deformed sediments south of the DFZ.

6.4. Timing of faulting and implications for Late Cenozoic tectonic evolution of the NE Bengal Basin

The study area has undergone a three-phase tectonics: *(i)* extension during the rifting of the Indian Plate from rest of the Gondwanaland – from Middle Jurassic, *(ii)* compression during the India-Eurasia collision – from Eocene-Oligocene transition, and *(iii)* transpression phase during the India-Mayanmar collision – from Miocene (Biswas et al., 2007b; Hossain et al., 2019, 2020c; Yang et al., 2020). Fault developed during rifting were reactivated and inverted during the India-Eurasia collision (Dasgupta et al., 2011; Kumar et al., 2012; Mishra et al., 2016). This uplifted the northern part of the basement and overlying sedimentary rocks to form a southward local slope facilitating a depocenter in the present-day Sylhet Trough. Later, the tectonic regime changed into transpression as the area experienced shortening from the east due to the India-Mayanmar oblique collision during Miocene (Biswas et al., 2007b). The inception of the Dauki and Oldham faults, and topographic growth of the Shillong plateau and Mikir Hills (Fig. 12) started devel-oping since Late Miocene/Early Pliocene by a transpression (Biswas et al. 2007a, 2007b; Govin et al., 2018).

Based on our results and structural synthesis, it is clear that the de-formations associated with the faults in the northeastern Sylhet Trough (i.e., Jaintiapur area, Sylhet) are genetically linked to the DFZ. Timing of the deformation and fault activation in the northeastern Sylhet Trough is inconclusive. However, the tectonic evolution of the Sylhet Trough is directly linked to the DFZ from the Mio-Pliocene to Holocene (Fig. 13). The Precambrian rocks of the Shillong plateau rose to the surface, and were consequently eroded at least since 5.2–4.9 Ma (Govin et al., 2018) due to the activation of the DFZ (Figs. 12–13). Records of
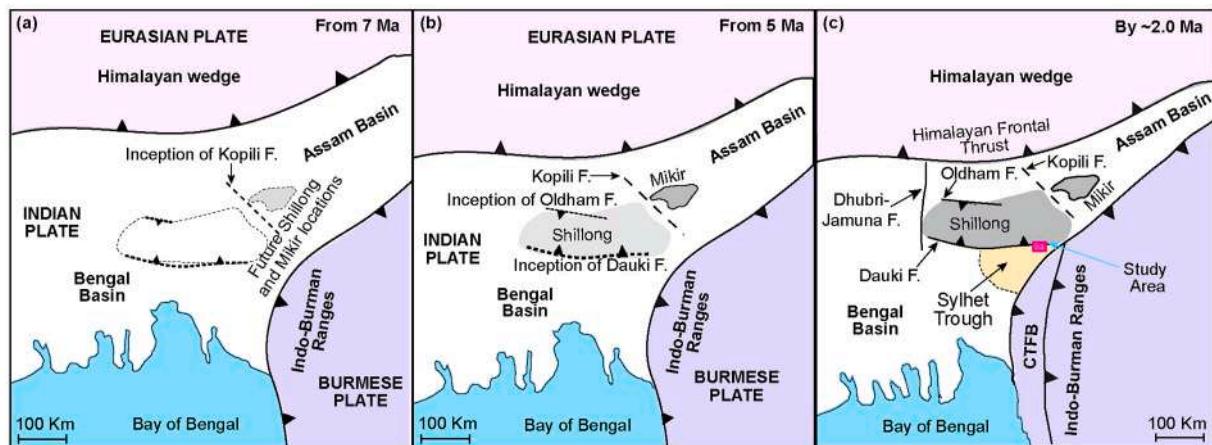
Fig. 12. Schematic diagrams showing the approximate timing of the Late Cenozoic tectonics of the Bengal and the Assam foredeep basins, and development of the major structures (modified after Govin et al., 2018). Inception of the Dauki and Oldham started first, which later developed the Shillong plateau and the Sylhet Trough.
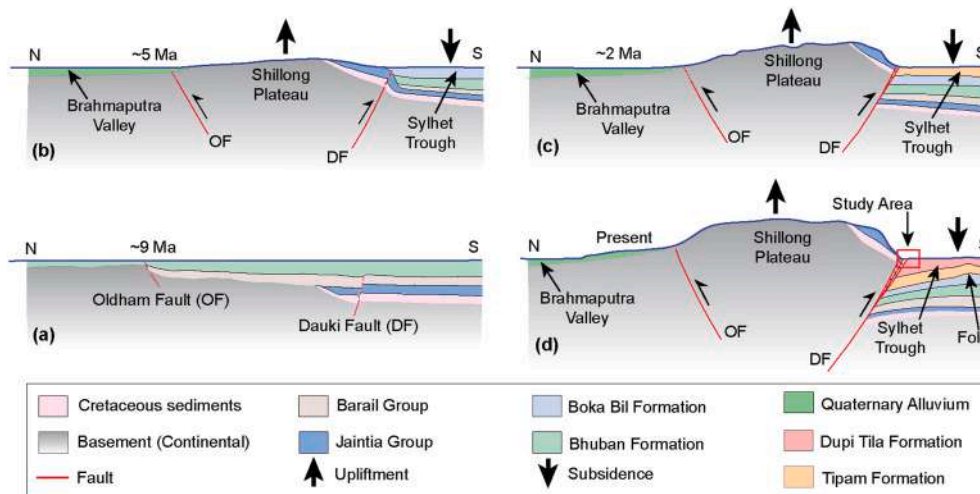
Fig. 13. A N–S Schematic cross-section showing the evolution (Figs. **a-d**) of the Dauki Fault Zone (DFZ) and its adjacent area (modified after Rosenkranz et al., 2018). Stratigraphy of the Sylhet Trough is based on Najman et al. (2016), and Khanam et al. (2021). Position and attitude of the Dauki and Oldham faults are after Bilham and England (2001), and Biswas et al. (2007a). Evidence of roll-over anticline has been observed in the marked study area position (Fig. d).

paleoseismicity, recent earthquakes, and modern geodetic measurements along the DFZ (Oldham, 1883, 1899; Bilham and England, 2001; Morino et al., 2011, 2014; Rajendran et al., 2017; Mallick et al., 2020) indicate that the study area and its adjoining region are still seismically active. The maximum principal stress axis trends ~ NNE in the west that changes to ~ ESE at east of the Sylhet Trough (Fig. 1a). The systematic clockwise deviation of maximum compressive stress thus affects the deformation across the region. The principal stress axes orientations derived from the fault-slip analysis in this study (Fig. 11b and c) match with the world stress map and with the GPS-derived present day stress field of the study area (Fig. 1a). Two major trends of the faults and their kinematics (Fig. 11a) are interrelated with the orientation of the maximum principal stress axis within the transpressive tectonic regime of the area. Studies suggest that a seismic gap exist in the eastern part of the DFZ (Steckler et al., 2018; Hossain et al., 2019). Consequently, the accumulated stress along the eastern segment of the DFZ can trigger large earthquake in this area.

7. Conclusions

The eastern segment of the Dauki Fault Zone (DFZ) displays deformation in the exposed Cenozoic successions in the NE Bengal Basin. Structurally, Jaintiapur and adjacent areas of Sylhet District is an east–west-trending monocline, which gently plunges to the west and reflects the prevailing stress field of the area. However, presence of opposite dipping beds in the Tama Bil area apparently suggests a local roll-over anticline. The roll-over is possibly related to the reverse drag of the footwall against the Dauki Fault. The deviations of the bedding strike from west to east in the study area are interpreted to be associated with the clock-wise bending of the DFZ within the area.

Local faults observed in the study area probably developed synchronously as well as through later strain partitioning of the DFZ. With respect to the DFZ, approximately E-W orientated local faults matches with the synthetic dextral Riedel shear structure. However, the mismatch of the NNW-SSW-oriented faults is possibly related to successive complex evolution of the study area due to clockwise rotation within the DFZ domains. The GPS-derived velocity field measurement and the principal stress axes orientation determined from the fault slip analysis are accorded the prevailing strain axis, and stress field of the study area.

The interpreted fault and fold system and the tectonic stress regime of the region will significantly improve the understanding of the already

proven petroleum system of the Sylhet Trough. Fold, fault bounded anticlines and transverse faults might be the possible hydrocarbon traps in the area. Evidence of paleoseismicity, recent earthquakes, and modern geodetic measurements along the DFZ suggest that the area is seismically active. Finally, this study is the first attempt to provide a comprehensive recording of the exposed deformation structures associated with the DFZ and would help to develop advanced kinematic and dynamic modelling of the DFZ in relation to the present day collision of the NE part of the Indian plate.

Declaration of competing interest

The authors declare that they have no known competing financial interests or personal relationships that could have appeared to influence the work reported in this paper.

Acknowledgements

Appendix A. Supplementary data

Supplementary data to this article can be found online at https://doi.org/10.1016/j.marpetgeo.2021.105133.

Credit author statement

Md. Sakawat HOSSAIN- fieldwork, data analyses, draft writing, Md. Sharif Hossain KHAN- fieldwork, data analyses, Rashed ABDULLAH- fieldwork, data analyses, Soumyajit MUKHERJEE- Significant amount of writing and finalization of the ms.

References

Alam, M., Alam, M.M., Curray, J.R., Chowdhury, M.L.R., Gani, M.R., 2003. An overview of the sedimentary geology of the Bengal Basin in relation to the regional tectonic framework and basin-fill history. Sediment. Geol. 155, 179–208.

Angelier, J., Baruah, S., 2009. Seismotectonics in Northeast India: a stress analysis of focal mechanism solutions of earthquakes and its kinematic implications. Geophys. J. Int. 178, 303–326.

Benavente, C., Zerathe, S., Audin, L., Hall, S.R., Robert, X., Delgado, F., Carcaillet, J., ASTER Team, 2017. Active transpressional tectonics in the Andean forearc of southern Peru quantified by [10]Be surface exposure dating of an active fault scarp. Tectonics 36 (9), 1662–1678.

Bilham, R., 2004. Earthquakes in India and the Himalaya: tectonics, geodesy and history. Ann. Geophys. 47, 839–858.

Bilham, R., England, P.C., 2001. Plateau "pop-up" in the great 1897 Assam earth-quake. Nature 410, 806–809.

Biswas, S., Coutand, I., Grujic, D., Hager, C., Stoeckli, D., Grasemann, B., 2007a. Exhumation and uplift of the Shillong plateau and its influence on the eastern Himalayas: new constraints from apatite and zircon (U-Th-[Sm])/He and apatite fission track analyses. Tectonics 26, TC6013. https://doi.org/10.1029/2007TC002125.

Biswas, S., Grasemann, B., 2005a. Quantitative morphotectonics of the southern Shillong plateau (Bangladesh/India). Austrian Journal of Earth Sciences 97, 82–93.

Biswas, S., Grasemann, B., 2005b. Structural modelling of the subsurface geology of the Sylhet trough, Bengal basin. Bangladesh Geoscience Journal 11, 19–33.

Biswas, S., Wiesmayr, G., Grasemann, B., 2007b. Development of a monocline in the northeast Sylhet trough along the Dauki Fault, NE Bangladesh. Geophys. Res. Abstr. 9, 00366. SRef-ID: 1607-7962/gra/EGU2007-A-00366.

Brandes, C., Tanner, D.C., 2014. Fault-related folding: a review of kinematic models and their application. Earth Sci. Rev. 138, 352–370.

Cardozo, N., Allmendinger, R.W., 2013. Spherical projections with OSXStereonet. Computers & geosciences, 51, 193–205.

Chowdhury, K.R., Biswas, S., Ahmed, A.M.M., 1996. The structural and tectonic set-up of Jaintiapur and adjacent areas, Sylhet District, Bangladesh. Bangladesh Geoscience Journal 2, 1–14.

Curiale, J.A., Covington, G.H., Shamsuddin, A.H.M., Morelos, J.A., Shamsuddin, A.K.M., 2002. Origin of petroleum in Bangladesh. AAPG (Am. Assoc. Pet. Geol.) Bull. 86 (4), 625–652.

Dasgupta, S., Pande, P., Ganguli, D., Iqbal, Z., Sanyal, K., Venkataraman, N.V., Dasgupta, S., Sural, B., Harendranath, L., Mazumdar, K., Sanyal, S., Roy, A., Das, L.

K., Misra, P.S., Gupta, H., 2000. In: Narula, P.L., Acharyya, S.K., Banerjee, J. (Eds.), Seismotectonic Atlas of India and its Environs. Geological Survey of India, Bangalore, p. 30.

Dasgupta, K., Samin, S., Bharali, B, R., 2011. An analysis of pre-tertiary plays in matimekhana-deohal area - a case study from OIL's operational area in northeast India. In: Search and Discovery Article #10303, AAPG International Conference and Exhibition. Alberta. Canada, Calgary. September 12-15.

Davison, I., Faull, T., Greenhalgh, J., Beirne, E.O., Steel, I., 2015. Transpressional structures and hydrocarbon potential along the Romanche Fracture Zone: a review. In: Nemčok, M., Rybár, S., Sinha, S.T., Hermeston, S.A., Ledvényiová, L. (Eds.), Transform Margins: Development, Controls and Petroleum Systems, vol. 431. Geological Society, London, Special Publications, pp. 235–248.

Dewey, J.F., Holdsworth, R.E., Strachan, R.A., 1998. Transpression and transtension zones, 1998. In: Holdsworth, R.E., Strachan, R.A., Dewey, J.F. (Eds.), Continental Transpressional and Transtensional Tectonics, vol. 135. Geological Society, London, Special Publications, pp. 1–14.

Dutta, D., Biswas, T., Mukherjee, S., 2019. Arc-parallel compression in the NW Himalaya: evidence from structural and palaeostress studies of brittle deformation from the clasts of the Upper Siwalik, Uttarakhand, India. Journal of Earth System Science 128, 125.

Dutta, D., Mukherjee, S., 2019. Opposite shear senses: geneses, global occurrences, numerical simulations and a case study from the Indian western Himalaya. J. Struct. Geol. 126, 357–392.

Dutta, D., Mukherjee, S., 2021. Extrusion kinematics of UHP terrane in a collisional orogen: EBSD and microstructure-based approach from the TsoMorariCrystallines (Ladakh Himalaya). Tectonophysics 880, 228641.

Erslev, E.A., 1991. Trishear fault-propagation folding. Geology 19, 617–620.

Evans, P., 1932. Tertiary succession in Assam. Trans. Min. Geol. Inst. India 27 (3), 155–260.

Gahalaut, V.K., Kundu, B., Laishram, S.S., Catherine, J., Kumar, A., Singh, M.D., Tiwari, R., Chadha, R., Samanta, S., Ambikapathy, A., 2013. Aseismic plate boundary in the Indo-Burmese wedge, northwest Sunda Arc. Geology 41 (2), 235–238.

Ghosh, G.K., Dasgupta, R., Reddy, B.J., Singh, S.N., 2015. Gravity data interpretation across the Brahmaputra thrust and Dauki Fault in the north-eastern India. J. Geophys. XXXVI, 31–38.

Goffey, G.P., Craig, J., Needham, T., Scott, R., 2010. Fold–thrust belts: overlooked provinces or justifiably avoided?. In: Goffey, G.P., Craig, J., Needham, T., Scott, R. (Eds.), Hydrocarbons in Contractional Belts, vol. 348. Geological Society, London, Special Publications, pp. 1–6.

Goscombe, B.D., Gray, D., Armstrong, R., Foster, D.A., Vogl, J., 2005. Event geochronology of the pan-african kaoko belt, Namibia. Precambrian Res. 140, 103–131.

Goscombe, B.D., Passchierb, C.W., Hand, M., 2004. Boudinage classification: end-member boudin types and modified boudin structures. J. Struct. Geol. 26, 739–763.

Govin, G., Najman, Y., Copley, A., Millar, I., van der Beek, P., Huyghe, P., Grujic, D., Davenport, J., 2018. Timing and mechanism of the rise of the Shillong plateau in the himalayan foreland. Geology 46 (3), 279–282.

Harris, L.B., Beeson, J., 1993. Gondwanaland significance of lower palaeozoic deformation in central India and SW western Australia. J. Geol. Soc. 150, 811–814. London.

Heidbach, O., Rajabi, M., Reiter, K., Ziegler, M., 2016. World Stress Map 2016. V. 1.1. GFZ Data Services.

Hiller, K., Elahi, M., 1984. Structural Development and Hydrocarbon Entrapment in Surma Basin, Bangladesh (Northeast Indo Burman Fold Belt). Proceeding of the 5th offshore South-East Asia Conference, Singapore.

Hossain, M.S., Chowdhury, K.R., Khan, M.S.H., Abdullah, R., 2016. Geotectonic settings of the Dauki Fault – a highly potential source for a significant seismic threat. In: Proceedings of International Conference Humboldt Kolleg on Living under Threat of Earthquake. Kathmandu, Nepal. Abstract: 25.

Hossain, M.S., Khan, M.S.H., Chowdhury, K.R., Abdullah, R., 2019. Synthesis of the tectonic and structural elements of the Bengal basin and its surroundings. In: Mukherjee, S. (Ed.), Tectonics and Structural Geology: Indian Context. Springer International Publishing AG, ISBN 978-3-319-99341-6, pp. 135–218.

Hossain, M.S., Khan, M.S.H., Chowdhury, K.R., Afrooz, M., 2014. Morpho-structural classification of the Indo-Burman Ranges and the adjacent regions. In: National Conference on Rock Deformation & Structures (RDS-III), Assam, India, p. 31. Abstract volume,.

Hossain, M.S., Khan, M.S.H., Abdullah, R., Chowdhury, K.R., 2020a. Tectonic development of the Bengal basin in relation to fold-thrust belt to the east and to the north. In: Biswal, T.K., Ray, S.K., Grasemann, B. (Eds.), Structural Geometry of Mobile Belts of the Indian Subcontinent. Springer Nature Switzerland AG, ISBN 978-3-030-40593-9, pp. 91–109.

Hossain, M.S., Rahman, M.M., Khan, R.A., 2020b. Active Seismic Structures, Energy Infrastructures, and Earthquake Disaster Response Strategy - Bangladesh Perspective. Int. Energy J. 20 (3A), 509–522. http://www.rericjournal.ait.ac.th/index.php/reric/article/view/2528.

Hossain, M.S., Xiao, W., Khan, M.S.H., Chowdhury, K.R., Ao, S., 2020c. Geodynamic model and tectono-structural framework of the Bengal Basin and its surroundings. J. Maps 16 (2), 445–458.

Johnson, S.Y., Alam, A.M.N., 1991. Sedimentation and tectonic of the Sylhet trough, Bangladesh. Geol. Soc. Am. Bull. 103, 1513–1522.

Katz, Y., Weinberger, R., Aydin, A., 2004. Geometry and kinematic evolution of Riedel shear structures, capitol reef national park, Utah. J. Struct. Geol. 26, 491–501.

Khan, M.S.H., Biswas, S., Singh, S., Pati, P., 2006. OSL choronology of Dihing Formation and recent upliftment rate along the Dauki Fault, NE Bangladesh. Bangladesh Geoscience Journal 12, 1–11.

Khan, M.S.H., Hossain, M.S., Islam, R., 2019. Geomorphology, structural model and active tectonics of the Rashidpur structure, Bengal Basin, Bangladesh. Bangladesh Geoscience Journal 25, 1–21.

Khan, M.S.H., Hossain, M.S., Uddin, M.A., 2018. Geology and active tectonics of the lalmai hills, Bangladesh – an overview from Chittagong Tripura Fold Belt perspective. J. Geol. Soc. India 92 (6), 713–720.

Khanam, F., Rahman, M.J.J., Alam, M.M., Abdullah, R., 2021. Sedimentation and basin-fill history of the neogene successions of Sylhet trough, Bengal basin, Bangladesh. Int. J. Earth Sci. https://doi.org/10.1007/s00531-020-01946-1.

Khattri, K.N., 1992. Semological investigation in northeastern region of India. In: Gupta, G.D. (Ed.), Himalayan Seismicity. Mem. Geol. Surv. Ind, pp. 275–302.

Kreemer, C., Blewitt, G., Klein, E.C., 2014. A geodetic plate motion and global strain rate model. G-cubed 15, 3849–3889.

Kumar, A., Mitra, S., Suresh, G., 2015. Seismotectonics of the Eastern Himalayan and indo-burman plate boundary systems. Tectonics 34, 2279–2295.

Kumar, T.S., Bharali, B.R., Verma, A.K., 2012. Basement Configuration and Structural Style in OIL's Operational Areas of Upper Assam. Search and Discovery Article #50739, GEO-India. Greater Noida, New Delhi, India. January 12-14. 2011.

Lin, S., Jiang, D., Williams, P.F., 1999. Discussion on transpression and transtension zones. In: Geological Society, London, Special Publications, vol. 135, pp. 1–14, 1998.

Lindsey, E.O., Almeida, R., Mallick, R., Hubbard, J., Bradley, K., Tsang, L.L.H., et al., 2018. Structural control on downdip locking extent of the Himalayan megathrust. J. Geophys. Res.: Solid Earth 123.

Mallick, R., Hubbard, J.A., Lindsey, E.O., Bradley, K.E., Moore, J.D.P., Ahsan, A., Alam, A.K.M.K., Hill, E.M., 2020. Subduction initiation and the rise of the Shillong plateau. Earth Planet Sci. Lett. 543, 116351.

Mallick, R., Lindsey, E.O., Feng, L., Hubbard, J., Banerjee, P., Hill, E.M., 2019. Active convergence of the India-Burma-sunda plates revealed by a new continuous GPS network. J. Geophys. Res.: Solid Earth 124, 3155–3171.

Marrett, R., Allmendinger, R.W., 1990. Kinematic analysis of fault-slip data. J. Struct. Geol. 12 (8), 973–986.

Maurya, D.M., Shaikh, M., Mukherjee, S., 2021. Structural attributes and paleostress analysis of Quaternary landforms along the Vigodi Fault (VF) in Western Kachchh region. Quat. Int. https://doi.org/10.1016/j.quaint.2021.04.029.

McClay, K.R., Insley, M.W., 1986. Duplex structures in the lewis thrust sheet, crowsnest pass, rocky mountains, alberta, Canada. J. Struct. Geol. 8, 911–922.

Meghraoui, M., Atakan, K., 2014. The contribution of paleoseismology to earthquake hazard evaluations. In: Wyss, M. (Ed.), Earthquake Hazard, Risk, and Disasters, ISBN 978-0-12-394848-9.

Meghraoui, M., Pondrelli, S., 2012. Active faulting and transpression tectonics along the plate boundary in North Africa. Ann. Geophys. 55 (5), 955–967.

Misra, A.A., Bhattacharya, G., Mukherjee, S., Bose, N., 2014. Near N-S paleo-extension in the western Deccan region in India: does it link strike-slip tectonics with India-Seychelles rifting? Int. J. Earth Sci. 103, 1645–1680.

Mishra, S.K., Phukon, J., Bhoktiari, P., Rahaman, A., 2016. Integrated structural analysis of fractured basement reservoir in the south Assam shelf, India. Proceeding of Indian National Science Academy 82 (3), 923–933.

Monsur, M.H., 2020. Quaternary Geology of Bangladesh, vol. 384p. Event Plus, Dhaka, Bangladesh, ISBN 978-984-34-9083-4.

Morino, M., Kamal, A.S.M.M., Akhter, S.H., Rahman, M.Z., Ali, R.M.E., Talukder, A., Khan, M.M.H., Matsuo, J., Kaneko, F., 2014. A paleo-seismological study of the Dauki fault at Jaflong, Sylhet, Bangladesh: historical seismic events and an attempted rupture segmentation model. J. Asian Earth Sci. 91, 218–226.

Morino, M., Kamal, A.S.M.M., Muslim, D., Ali, R.M.E., Kamal, M.A., Rahman, M.Z., Kaneko, F., 2011. Seismic event of the Dauki Fault in 16th century confirmed by trench investigation at gabrakhari village, haluaghat, mymensingh, Bangladesh. J. Asian Earth Sci. 42, 492–498.

Mulchrone, K.F., Mukherjee, S., 2015. Shear senses and viscous dissipation of layered ductile simple shear zones. Pure Appl. Geophys. 172, 2635–2642.

Mukherjee, S., 2014. Review of flanking structures in meso- and micro-scales. Geol. Mag. 151, 957–974.

Mukherjee, S., 2019. Particle tracking in ideal faulted blocks using 3D co-ordinate geometry. Mar. Petrol. Geol. 107, 508–514.

Najman, Y., Bracciali, L., Parrish, R.R., Chisty, E., Copley, A., 2016. Evolving strain partitioning in the eastern Himalaya: the growth of the Shillong plateau. Earth Planet Sci. Lett. 433, 1–9.

Nandy, D.R., 2001. Geodynamics of Northeastern India and Adjoining Region. ABC Publication, Kolkata, India, p. 209.

Nemčok, M., Rybár, S., Sinha, S.T., Hermeston, S.A., Ledvényiová, L., 2016. Transform margins: development, controls and petroleum systems – an introduction. In: Geological Society, London, Special Publications, vol. 431, pp. 1–38.

Nielsen, C., Chamot-Rooke, N., Rangin, C., ANDAMAN Cruise Team, 2004. From partial to full strain partitioning along the Indo-Burmese hyper-oblique subduction. Mar. Geol. 209 (1–4), 303–327.

Oldham, T., 1883. A Catalogue of Indian Earthquakes, vol. 19. Memories of the Geological Survey of India, Calcutta, pp. 163–215.

Oldham, R.D., 1899. Report of the great earthquake of 12th June 1897. Memoir. Geol. Surv. India 29, 379p. Reprinted by: Geological Survey of India, Calcutta, 1981.

Panda, D., Kundu, B., Santosh, M., 2018. Oblique convergence and strain partitioning in the outer deformation front of NE Himalaya. Nature 8, 10564.

Rahman, M.J.J., Xiao, W., Hossain, M.S., Yeasmin, R., Sayem, A.S.M., Ao, S., Yang, L., Abdullah, R., Dina, N.T., 2020. Geochemistry and detrital zircon U-Pb dating of pliocene-pleistocene sandstones of the Chittagong Tripura Fold Belt (Bangladesh): implications for provenance. Gondwana Res. 78, 278–290.

Rajendran, K., Parameswaran, R.M., Rajendran, C.P., 2017. Seismotectonic perspectives on the Himalayan arc and contiguous areas: inferences from past and recent earthquakes. Earth Sci. Rev. 173, 1–30.

Reimann, K.U., 1993. Geology of Bangladesh. Gebrueder Borntraeger, Berlin, 3443110207 9783443110208.

Reitz, M.D., Pickering, J.L., Goodbred, S.L., Paola, C., Steckler, M.S., Seeber, L., Akhter, S.H., 2015. Effects of tectonic deformation and sea level on river path selection: theory and application to the Ganges-Brahmaputra-Meghna River Delta. J. Geophys. Res. Earth Surf. 120, 671–689.

Rosenkranz, R., Schildgen, T., Wittmann, H., Spiegel, C., 2018. Coupling erosion and topographic development in the rainiest place on Earth: reconstructing the Shillong Plateau uplift history with in-situ cosmogenic^{10}Be. Earth Planet Sci. Lett. 483, 39–51.

Sarker, M.H., Akter, J., 2011. Evolution of rivers in subsiding Sylhet basin: northeast of Bangladesh. In: Advances in River Science 2011 (Swansea, United Kingdom).

Sarmah, S.K., Deka, D.K., Deka, S., 1992. Micro-earthquake survey in lower Assam region. In: Gupta, G.D. (Ed.), Himalayan Seismicity. Mem. Geol. Surv. Ind, pp. 303–318.

Shaikh, M., Maurya, D.M., Mukherjee, S., Vanik, N., Padmalal, A., Chamyal, L., 2020. Tectonic evolution of the intra-uplift Vigodi-Gugriana-Khirasra-Netra Fault System in the seismically active Kachchh Rift Basin, India: implications for the western continental margin of the Indian plate. J. Struct. Geol. 140, 104124.

Shamsuddin, A.H.M., Abdullah, S.K.M., 1997. Geological evolution of the Bengal Basin and its implication in hydrocarbon exploration in Bangladesh. Indian J. Geol. 69, 93–121.

Steckler, M.S., Mondal, D., Akhter, S.H., Seeber, L., Feng, L., Gale, J., 2016. Locked and loading megathrust linked to active subduction beneath the Indo-Burman ranges. Nat. Geosci. 9, 615–618.

Steckler, M.S., Stein, S., Akhter, S.H., Seeber, L., 2018. The wicked problem of earthquake hazard in developing countries. Earth and Space Science News. https://doi.org/10.1029/2018EO093625.

Stein, S., Wysession, M., 2003. An Introduction to Seismology, Earthquakes, and Earth Structure. Blackwell Science, Oxford, p. 498.

Swanson, M.T., 1988. Pseudotachylyte-bearing strike-slip duplex structures in the Fort Foster brittle zone, S. Maine. J. Struct. Geol. 10, 813–828.

Vanik, N., Shaikh, H., Mukherjee, S., Maurya, D.M., Chamyal, L.S., 2018. Post-Deccan trap stress reorientation under transpression: evidence from fault slip analyses from SW Saurashtra, western India. J. Geodyn. 121, 9–19.

Vernant, P., Bilham, R., Szeliga, W., Drupka, D., Kalita, S., Bhattacharyya, A.K., Gaur, V. K., Pelgay, P., Cattin, R., Berthet, T., 2014. Clockwise rotation of the Brahmaputra valley relative to India: tectonic convergence in the eastern Himalaya, Naga hills, and Shillong plateau. J. Geophys. Res.: Solid Earth 119.

Yadav, R., Tiwari, V.M., 2018. Numerical simulation of present day tectonic stress across the Indian subcontinent. Int. J. Earth Sci. 107, 2449–2462.

Yang, L., Xiao, W., Rahman, M.J.J., Windley, B.F., Schulmann, K., Ao, S., Zhang, J., Chen, Z., Hossain, M.S., Dong, Y., 2020. Indo-Burma passive amalgamation along kaladan fault: insights from provenance of Chittagong-Tripura Fold Belt (Bangladesh). Geol. Soc. Am. Bull. 132 (9–10), 1953–1968.

Yeats, R.S., Sieh, K., Allen, C.R., 1997. The Geology of Earthquakes, p. 568p. Oxford UniversityPress.

Yin, A., Dubey, C.S., Webb, A.A.G., Kelty, T.K., Grove, M., Gehrels, G.E., Burgess, W.P., 2010. Geologic correlation of the Himalayan orogen and Indian craton: Part 1. Structural geology, U-Pb zircon geochronology, and tectonic evolution of the Shillong Plateau and its neighboring regions in NE India. Geol. Soc. Am. Bull. 122 (3–4), 336–359.